

**Flood Susceptibility Mapping using GIS and Remote Sensing
data through Multi Criteria Decision Analysis: A case study of District
Khairpur, Sindh.**



By

Afaq Rais

(2019-NUST-MS-GIS-320006)

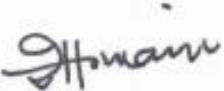
**A thesis submitted in partial fulfillment of the requirements for the
degree of Master of Science in Remote Sensing and GIS**

**Institute of Geographical Information Systems
School of Civil and Environmental Engineering
National University of Sciences & Technology
Islamabad, Pakistan**


August 2023


CERTIFICATE

Certified that final copy of MS/MPhil thesis written by Afaq Rais (Registration No. MSRSGIS 00000320006), of Session 2019 (Institute of Geographical Information systems) has been vetted by undersigned, found complete in all respects as per NUST Statutes/Regulation, is free of plagiarism, errors, and mistakes and is accepted as partial fulfillment for award of MS/MPhil degree. It is further certified that necessary amendments as pointed out by GEC members of the scholar have also been incorporated in the said thesis.

Signature: 
Name of Supervisor: Dr Ejaz Hussain
Date: 30.08.2023
Dr. Ejaz Hussain
Associate Professor
Institute of Geographical Information Systems (IGIS), NUST

Signature (HOD): 
Date: 30/08/2023
Dr. Javed Iqbal
Professor & HOD IGIS, SCEE (NUST)
H-12, Islamabad

Signature (Associate Dean): 
Date: 30.8.2023
Dr. Ejaz Hussain
Associate Dean
Institute of Geographical Information Systems (IGIS), NUST

Signature (Principal & Dean SCEE): 
Date: 31 AUG 2023
PROF DR MUHAMMAD IRFAN
Principal & Dean
SCEE, NUST

ACADEMIC THESIS: DECLARATION OF AUTHORSHIP

I, **Afaq Rais**, declare that this thesis and the work presented in it are my own and have been generated by me as the result of my own original research.

“Flood susceptibility mapping using GIS and remote sensing data through Multi Criteria Decision Analysis: A case study of District Khairpur, Sindh”

I confirm that.

1. This thesis is composed of my original work, and contains no material previously published or written by another person except where due reference has been made in the text.
2. Wherever any part of this thesis has previously been submitted for a degree or any other qualification at this or any other institution, it has been clearly stated.
3. I have acknowledged all main sources of help.
4. Where the thesis is based on work done by myself jointly with others, I have made clear exactly what was done by others and what I have contributed myself.
5. None of this work has been published before submission.
6. This work is not plagiarized under the HEC plagiarism policy.

Signed.

Date.

DEDICATION

“Dedicated to my Family who support me in all moments of life”

and

“To teachers and friends who helped me to complete my thesis”

ACKNOWLEDGEMENTS

All praises to almighty Allah who to whom everything belongs and to whom we all will return. First, I would like to give special thanks to my supervisor Dr. Ejaz Hussain for his continuous support, advice, comments, and feedback throughout my research period. He always helped me when I needed it and his guidance and support in this study was inimitable. I am grateful for the support he gave whenever I faced some challenges.

I would like to thank my examination committee members Dr. Muhammad Azmat, Mr. Naqash Taj Abbasi and Dr. Hamza Farooq Gabriel. The support, guidance and suggestions helped me a lot. I am also thankful to the NUST and all administration, which allowed me to do research in this developing and growing field.

Finally, my gratitude to my parents for their trust in me and providing me with moral and financial support to acquire my ambition, I just can't thank them enough. Also, my appreciation goes to the rest of my family and friends for putting me in their prayers.

Afaq Rais

TABLE OF CONTENTS

CERTIFICATE	i
ACADEMIC THESIS. DECLARATION OF AUTHORSHIP	ii
DEDICATION	iii
ACKNOWLEDGEMENTS	iv
LIST OF FIGURES	vii
LIST OF TABLES	viii
LIST OF ABBREVIATIONS.....	ix
ABSTRACT	x
Chapter 1: INTRODUCTION	1
1.1 Background	1
1.2 Climate Change and Flooding.....	3
1.3 Economic impacts of the floods in Pakistan	5
1.4 Flood Management in Pakistan	6
1.5 Literature Review	7
1.6 Problem Statement	11
1.7 Objectives.....	11
Chapter 2: MATERIAL AND METHODS	12
2.1 Study Area	12
2.2 Datasets	12
2.3 Landsat Data.....	15
2.4 Digital Elevation Model	15
2.5 Meteorological Data	17
2.6 River Network.....	17
2.7 Geology data	17
2.8 Soil data.....	18
2.9 Flood Inventory	18
2.10 Methodology.....	20
2.10.1 Geospatial layers for flood susceptibility mapping.....	20
2.10.2 Flood causative factors.....	20
2.10.3 Accuracy Assessment.....	23
2.11 Modelling Approach	24
2.11.1 Analytic Hierarchy Process (AHP)	24
2.11.2 Frequency Ratio	25

2.11.3	Shannon’s Entropy	26
Chapter 3:	RESULTS AND DISCUSSIONS	28
3.1	Flood Causative Factors	28
3.1.1	Elevation.....	28
3.1.2	Slope.....	28
3.1.3	Curvature	29
3.1.4	Topographic Wetness Index	29
3.1.5	Normalized Difference Vegetation Index.....	29
3.1.6	Normalized Difference Water Index	32
3.1.7	Land Use Land Cover	32
3.1.8	Distance to stream	32
3.1.9	Average Annual Rainfall	32
3.1.10	Soil	35
3.1.11	Geology	35
3.2	Frequency Ratio Model.....	35
3.3	Shannon’s Entropy Model.....	39
3.4	Analytical Hierarchy Process	45
3.5	Weight Linear Combination Approach	45
3.6	Validation of The Flood Susceptibility Maps.....	52
Chapter 4:	CONCLUSION AND RECOMMENDATIONS.....	56
4.1	Conclusion.....	56
4.2	Recommendations	57
REFERENCES.....		61

LIST OF FIGURES

Figure 1.1. An aerial view of Khairpur, Pakistan under flooding on August 30, 2022 (daily Dawn)	4
Figure 2.1. Map of study area map of district Khairpur Sindh.	13
Figure 2.2. Shuttle radar topography mission 30m digital elevation model of study area.	16
Figure 2.3. Landsat 9 image of October 2022.	16
Figure 2.4. Flow chart of methodology.	21
Figure 2.5. Flood inventory map.	22
Figure 3.1. Elevation map of the study area.	30
Figure 3.2. Slope map of the study area.	30
Figure 3.3. Curvature map of the study area.	31
Figure 3.4. Topographic wetness index map of the study area.	31
Figure 3.5. Normalized difference vegetation index of the study area.	33
Figure 3.6. Normalized difference water index of the study area.	33
Figure 3.7. Land Use Land Cover of the study area.	34
Figure 3.8. Distance to stream map of the study area.	34
Figure 3.9. Average annual rainfall map of the study area.	36
Figure 3.10. Soil texture map of the study area.	36
Figure 3.11. Geological map of the study area.	37
Figure 3.12. Flood susceptible zones using frequency ratio.	40
Figure 3.13. The calculated area of flood susceptibility zones.	40
Figure 3.15. The calculated area of flood susceptibility zones.	46
Figure 3.14. Flood susceptible zones using shannon’s entropy.	46
Figure 3.16. Distribution of flood susceptibility areas.	53
Figure 3.17. Flood susceptible zones using analytical hierarchy process model.	53
Figure 3.19. Area under curve representing quality of shannon entropy model.	54
Figure 3.18. Area under curve representing quality of frequency ratio model.	54
Figure 3.20. Area under curve representing quality of analytical hierarchy process model.	55

LIST OF TABLES

Table 1.1. The record of floods in Pakistan from 1950 to 2022 (Khan et al, 2021; NDMA, 2022).	4
Table 2.1. Summary of the data used.	14
Table 2.2. Meteorological Ground Stations information.	19
Table 2.3. Brief description of all the land use landcover types.	19
Table 2.4. Classification of area under curve range.	22
Table 3.1. Frequency Ratio for each class of each parameter.	41
Table 3.2. Shannon’s entropy weights for each parameter.	47
Table 3.3. Shows pair wise comparison matrix.	50
Table 3.4. Shows weightages of normalized factors.	51
Table 3.5. Area under curve values of models.	55

LIST OF ABBREVIATIONS

Abbreviation	Explanation
ETM+	Enhanced Thematic Mapper Plus
GIS	Geographic Information System
LULC	Land use Land cover
NDVI	Normalized Difference Vegetation Index
PMD	Pakistan Meteorological Department
USGS	United States Geological Survey
SRTM	Shuttle Radar Topography Mission
FR	Frequency Ratio
SE	Shannon's Entropy
UTM	Universal Transverse Mercator
WGS	World Geodetic System
NDWI	Normalized Difference Water Index
FFC	Federal Flood Commission

ABSTRACT

One of the biggest natural disasters is flooding, frequently occurring in Pakistan, due to the excessive rainfall in monsoon and the climate change. These floods cause severe damage to physical and anthropogenic resources. Identification and mapping of flood susceptible areas is essential for rescue, relief, rehabilitation, and timely management related informed decision-making. Creating flood susceptibility maps and conducting assessments are essential elements of flood prevention and mitigation strategies. Geographic Information System (GIS) and remote sensing data are valuable resources for mapping flood susceptibility at different spatial scales. This study focused on utilizing remote sensing data and GIS to evaluate Frequency Ratio Model (FR), Shannon's Entropy (SE) and Analytical Hierarchy Process (AHP) for the identification and mapping of flood susceptible areas in District Khairpur of Sindh Province. Eleven flood causative parameters were considered for flood susceptibility mapping. The results validation was based on the comparison of the historical flood susceptible zones using Area Under Curve (AUC) Method. The results reveal that precipitation, distance to stream, and soil are the most significant factors in flood generation and elevation is the least. The AUC values were 90.7%, 87.6%, and 79.5% for the FR, SE, and AHP models, respectively. These values indicate that FR model provides the highest accuracy and better results compared to SE and AHP. The results highlight the potential of remote sensing data for generating flood susceptibility maps and their use to devise effective mitigation and formulate efficient flood management plans.

INTRODUCTION

1.1 Background

Flood refers to the overflow of water bodies beyond their regular boundaries, or the buildup of water over land that is otherwise not typically inundated (Kundzewicz, 2014). Floods are a natural hazard that could be destructive for both the humans and the natural environment. It affects developed and underdeveloped countries. Floods are approximately 40% of all the natural disasters (Molla, 2011).

Because of global climate change, natural catastrophes such as storms, droughts, tornadoes, tsunamis, and floods occur more frequently (Samu and Kentel, 2018). The effects of climate change have only recently begun to be understood as a hazard to the entire globe. This event might lead to changes in climatic zones, sea level rise, and rainfall patterns, among other things (Khan et al, 2021). One of the most expensive and pervasive climate-related natural disasters is flooding. It was projected that floods killed 539,000 people between 1980 and 2009 and negatively impacted the lives of 2.8 billion people (Eccles et al, 2019). In South Asia, a warmer climate is very likely to lead to an increase in flooding's frequency, extent, and magnitude (Mirza, 2010). The areas most impacted by climate change, including Pakistan, are the developing economies, more susceptible to climatic hazards (Khan et al, 2021).

The combination of several physical processes results in flooding. These include meteorological factors such as the amount, intensity, and distribution of rainfall, hydrological preconditions such as soil saturation and snow cover, runoff generating process such as infiltration and runoff on hillslopes, and river routing such as the superposition of flood waves (Nied et al, 2014).

There are different types of floods caused by different factors. including 1) Flash Floods caused by heavy rainfalls. These floods occur when the high rainfall cannot be dispersed by soil absorption, runoff, and drainage. These floods occur in a very short period, generally 2 to 6 hours (Marchi et al, 2010). 2) Riverine (Fluvial) floods occur when a river exceeds its capacity due to intense rainfall over an extended period. More and more water is added into a river and at a specific time the river exceeds its capacity and water starts flowing out of the river. Glacial melting also contributes to riverine floods (Weissmann et al, 2010). 3) Reservoir flooding occurs due to structural failure. However, such events are very rare. In one such event when the Shadi Kor dam in Pasni burst on February 11, 2005, more than 135 people perished (Danso-Amaoko et al, 2012). 4) Storm surges take place when tidal waves are elevated above their normal height in the coastal region due to severe force of wind caused by low pressure in the open ocean (Wahl et al, 2015).

According to (Tariq and Giesen, 2012), three different meteorological systems have an impact on the precipitation in catchments that cause floods in Pakistan. The most significant of these meteorological systems are 1) the monsoon depression, which originates in the Bay of Bengal. 2) Mediterranean Sea waves originating from the west (winter rains). 3) Seasonal lows (cyclones) from the Arabian Sea.

Pakistan has experienced terrible floods since its creation. Both economic and human losses from the flood had been significant. Millions of people become homeless, and thousands lost their lives. In Pakistan, heavy monsoon rains and glacier melting are the main causes of floods. Due to Pakistan's location inside the most active monsoon belt, this region experiences tremendous rainfall intensity. The July 2010 flood is regarded as the worst in Pakistan history. Nearly 2000 individuals lost their lives and affected more than 20 million people (Deen, 2015). A disastrous heat wave in May 2022 and flood in August 2022 in Pakistan had a disproportionately negative impact in the southern areas. This flood had an impact on a

population equivalent to one-third of the world's fifth-most populous country, which displaced 32,000,000 and killed 1,486 people, including 530 children (NDMA, 2022).

1.2 Climate Change and Flooding

South Asia is most prone to floods. Flooding in the area is due to heavy monsoon rain, which seriously harms people, crops, property, and infrastructure. Extreme floods are happening more frequently in Bangladesh, India, and Pakistan. However, while past extreme flooding is within the range, future flooding in South Asia may increase in frequency, magnitude, and extent due to climate variability. In many parts of the world, increased precipitation intensity is anticipated to increase the frequency and size of flood events. Most of the world's extreme precipitation events are expected to become more intense because of climate change (Eccles et al, 2019). Because the air over land would warm more than the air over oceans in the summer, producing an intense monsoon. Most climate models predict that precipitation will increase during the summer (Mirza, 2010).

The structure and operation of aquatic ecosystems, including wetlands, lakes, rivers, and coastal systems, are seriously threatened by human-induced climate change, altering the predominant precipitation patterns and runoff. To upset the equilibrium of water and sediment flux in river channels, humans have significantly altered the landscape. Due to alterations in the utilization of land (agricultural, urbanization), waterways receive more water (Poff, 2002).

Three different meteorological systems have an impact on the precipitation in catchments that cause floods in Pakistan. Typically, the monsoon season starts in June, reaches its peak in August, and ends in September. The monsoon rainy season gives an average rainfall of roughly 600 mm to 1,000 mm annually. While the daily maximum temperature during June exceeds 40°C, the average day time temperature in December and January is quite

Table 1.1. The record of floods in Pakistan from 1950 to 2022 (Khan et al, 2021; NDMA, 2022).

Period	Flood frequency	Economic loss US (Million \$)	Total affected population	Total deaths
1950-1959	6	1719	36,954	3691
1960-1969	2	33	224,427	32
1970-1979	5	116.5	13,637,200	2066
1980-1989	7	1367	1,304,900	519
1990-1999	14	1092.2	18,148,606	4180
2000-2009	33	706.14	9,574,150	2265
2010-2019	30	18.113	36,495,066	4712
2022	N/A	30000	33,046,329	1486



Figure 1.1. An aerial view of Khairpur, Pakistan under flooding on August 30, 2022 (daily Dawn)

near to 0 °C. Between July and September, humidity keeps the temperature only a little bit moderate (Ahmad et al, 2010).

The economy, cultures, aquatic and terrestrial ecosystems could all face significant consequences because of extreme precipitation amplification (Tabari, 2020).

1.3 Economic impacts of the floods in Pakistan

Natural climate related risks may quickly affect economic growth and market performance because they interact directly with key macroeconomic factors. As evidenced by the recent floods and their severe effects on Pakistan, one of the most catastrophic natural calamities is floods. It adversely impacts public health, causes unemployment, destroys the ecosystem, and has an adverse impact on socioeconomic conditions (Manzoor et al, 2022).

In Pakistan, the monsoon season of 2010 (July and August) caused the largest floods ever reported. In the country's north and northwest, flash floods were a result of heavy rains. The ensuing runoff created a mass of water heading south was about the size of the United Kingdom. The Munda and Amandara Headworks, the two prominent irrigation infrastructures, were extensively damaged by the record flood peaks in the Swat River, caused by the torrential rainfall in Khyber Pakhtunkhwa. After passing through Punjab and Kotri Barrage Sindh, the floodwaters continued downstream till they reached the Arabian Sea. Several important irrigation canals that use the Indus River to irrigate agricultural regions were affected. Heavy rains added to the problem, and water was diverted to agricultural land to avert flooding of the cities. (Asian Development Bank, 2010). Around 20 million people were forced to leave their homes, and about 50,000 square km of land was flooded. Standing crops, infrastructure, and land were all severely damaged (Robert Looney, 2012).

Since the middle of June 2022, Pakistan has seen numerous periods of intense monsoonal precipitation, which was mostly intensified by the intense-low pressure system. In

Pakistan, heavy rains are also linked to the presence of La Nina. Over \$30 billion is the projected economic losses. Famine is impending because of widespread agriculture losses and likely disease outbreaks in makeshift shelters (Nanditha, 2023).

According to (Mirza, 2010), most diseases that are common during the flood season, such as diarrhea, dysentery, and dengue are water related. The pathogens can infect people by contact or drinking contaminated water. Large coastal communities are being displaced, which affects public health by increasing the dispersion of infections, mortality, and bad health.

From years 1972 to 2013, (Sardar et al, 2016) evaluated how disasters affected Pakistan's Gross Domestic Product (GDP) growth and discussed three hazards associated with floods including: property devastation, death, and non-fatal communal outcomes. Their findings demonstrated that disaster preparedness and per capita GDP growth lessen the severity of the associated flood hazards.

Conceptually, the costs to the nation's economy can be divided into several categories, mostly based on the types of expenses (direct and indirect) and the time periods under consideration (immediate, short-run, medium-term, and long-run). Better infrastructure, warning systems, and preventative and protective measures in flood-prone areas could be made available to citizens with increased GDP growth (Manzoor et al, 2022).

1.4 Flood Management in Pakistan

In Pakistan, flooding happens frequently. However, the floods in Pakistan in 2010, 2011, 2012, 2014, and 2022 are typical examples, which have a significant impact on the livelihood of the population and the nation's GDP. Gilgit-Baltistan and some areas of the Sindh and Punjab provinces are highly flood prone (Khan et al, 2021).

Pakistan confronts the threat of rising irrigation water scarcity and is prone to flood hazards despite significant expenditures in its water sector over the past 50 years (World Bank,

1994). The country's primary source of irrigation water and flood risk is the Indus River and its five tributaries (Mustafa, 2002). (Rahmati, Flood susceptibility mapping using frequency ratio and weights-of-evidence models in the Golastan Province, Iran, 2015) (Rahmati, Flood susceptibility mapping using frequency ratio and weights-of-evidence models in the Golastan Province, Iran, 2015)

Flood management strategies, preparedness, and pre-flood measures are currently the three main strategies that the nation uses to manage (Ayaz et al, 2014). As a result of the frequent flood events, the government created a variety of flood protection programmes (Sayers et al, 2013). Following the creation of the “Federal Flood Council” in 1977, flood executives have been creating flood management strategies while using lessons from prior experiences at the local and federal levels. A strategy for long-term flood protection was developed in 1978. The "10-year National Flood Protection Plan" (NFFP), was implemented in several stages. Both the structural and non-structural flood management and planning strategies are being changed by the government. While non-structural methods include the use of meteorological and flood forecasting technologies to improve the rainfall data collection and monitoring watershed flows. Whereas structural interventions focus on the channelization of rivers and the construction of minor dams. To minimize losses during floods, non-structural methods also include the design of flood warning systems. In order to create flood forecasts and alerts, the Flood Forecasting Division of the “Pakistan Meteorological Department (PMD)” gathers hydro-meteorological data from numerous local, regional, and global sources. To prevent rumors and false information regarding floods, the chief meteorologist is solely responsible for the distribution of flood warnings (Tariq and Giesen, 2012).

1.5 Literature Review

Natural catastrophes including floods, droughts, tsunamis, hurricanes, and tornadoes are becoming more frequent due to climate change (Samu and Kentel, 2018). According to (Khan et al, 2021), climate change has gained attention as a worldwide danger in recent decades as its slow-moving effects have become apparent. These effects take many different forms, such as changing rainfall patterns, increasing sea levels, and changes in climatic zones.

According to a study conducted by (Vojtek et al, 2019), Floods are complicated occurrences that involve several dimensions, including geographical and temporal. Geographic Information Systems (GIS) have been shown to be useful tools for combining various data and factors, for producing flood vulnerability maps of by using logical and mathematical correlations. Different methods have been developed and used in various geographic locations to detect and assess areas that are vulnerable to floods. These techniques seek to efficiently identify and evaluate a location's susceptibility to flooding, supporting efforts at preparedness and mitigation.

In their study, (Liuzzo et al, 2019) focused on evaluating flood susceptibility, which refers to the degree of vulnerability to potential damage caused by water-related hazards. For successful land planning and management as well as quick and effective emergency responses, it is essential to identify regions that are vulnerable to floods. Researchers have greatly improved the ability to identify flood-prone areas by adding GIS into hydrologic research. This has made it easier to create precise flood susceptibility maps.

Hammami et al, (2019) commented that Multi Criteria Decision Analysis (MCDA) methodology has established itself as a useful tool for examining complex choice issues across diverse research fields. To enable well-informed decision-making, MCDA integrates a variety of criteria, including technological, environmental, and socioeconomic variables. MCDA was used in conjunction with GIS to precisely identify and map areas vulnerable to floods, utilizing

a thorough strategy that incorporates multiple elements. Study performed by (Das, 2020) mentions that many environmental factors, including topography, land use, geology, climate, and hydrological parameters, might affect the likelihood of a flood. Due to the intricacy of the decision-making process, these considerations are essential in the creation of flood susceptibility maps. To examine and address the complex decision processes incorporating numerous criteria, the study emphasizes the need of using a MCDA.

Balogun et al, (2022) investigated the effectiveness of Remote Sensing (RS) and GIS as potent tools for managing natural disasters. Many researchers have successfully used RS and GIS to assess flood catastrophe, flood susceptibility, produced flood risk maps, and effectively manage post-disaster scenarios. Flood susceptibility mapping has been further improved by the integration of Multi-Criteria Decision-Making (MCDM) models with GIS, allowing thorough analyses and well-informed decision-making in flood-prone regions.

Wang et al, (2021) states that large amount of rainfall is often brought in by climate change and global warming, which causes devastating floods. They used two distinct models and four hybrid models to analyze the geographical distribution of flood vulnerability in a specific area. Bivariate statistical models based on the Frequency Ratio (FR) and Index of Entropy were used as independent models. On the other hand, hybrid models merged statistical methods with the categorization and regression trees (CART) and multi-layer perception (MLP) models. The MLP-PD hybrid model had the greatest values for numerous specificity and accuracy metrics, as well as for success rates (AUC = 0.954), prediction rates (AUC = 0.949) and delivered the most effective performance.

Islam et al, (2021) conducted a study in the Lower Bagmati basin, “Shannon's Entropy”, a well-known model in landslide and groundwater mapping, which has emerged as a potential strategy in flood susceptibility mapping. The identification of flood-prone regions and high-

risk flood zones is made feasible by the efficient use of this approach. This information can help develop an early warning and emergency response system, facilitate early planning, and lessen the negative impacts of floods in the area.

Khosravi et al, (2016) performed a study on Bivariate statistical models, in particular the “FR” model, which was shown to be particularly well suited for vast study regions with sparse data and too simple to apply in a GIS. This model assumption of equal weights for various affecting elements is a drawback. The researchers suggested using Shannon's entropy technique, which solves the equal weighting problem, to deal with this issue. By using this method, all the models' outputs were rated outstanding, indicating their potential for usage in the Haraz Watershed, Mazandaran Province, in land use planning and flood control. Another research by (Liuzzo et al, 2019) emphasized the extensive usage of the FR model for a variety of tasks, including groundwater potential mapping, flood and landslide susceptibility mapping, and risk assessment for forest fires.

Msabi et al, (2021) said that a qualitative tool used in MCDM to aid in decision-making is the “Analytical Hierarchy Process” (AHP). The ability to prioritize and give weights to various criteria depends on expert knowledge. The identification of viable locations for residential, public, and industrial growth depends critically on flood susceptibility mapping in urban planning. Additionally, identifying flood-prone areas in the Dodoma region is required for efficient flood management strategies, mitigation, and prevention. In a study by (Swain et al, 2020), the AHP technique was identified as the most preferred approach, as it provided a specialized decision-making framework specifically tailored for flood susceptibility mapping. In AHP, flood vulnerability factors are ranked based on their importance to support informed decision-making processes.

In the study conducted by (Rahmati et al, 2015), the primary objective of flood susceptibility analysis was to identify regions that could be affected by impending floods. Therefore, it was decided to validate the resultant flood susceptibility maps by comparing them against flood events that were not used during the creation or training of the model, independent of the specific technique used for integrating the data. These abandoned flood zones were utilized to evaluate and confirm the veracity and correctness of the flood susceptibility maps.

1.6 Problem Statement

Due to the recent year floods in Pakistan, vast area was flooded yielding heavy losses both physically and anthropogenically. As Pakistan is going through an economic crisis the traditional methods of flood monitoring require a lot of financial resources and time. In such a case, RS technology is a cost effective and a viable resource and alternative. Identification of the flood susceptible areas using latest technologies can help improve mitigation reform, applied to minimize the damages in case of re-occurrence, and with least manual efforts and financial requirement.

This research explored and analyzed the areas that are susceptible to flooding in District Khairpur of Sindh and tried to suggest viable solutions that can help minimize or even negate the losses in the foreseeable future.

1.7 Objectives

- a) To assess, map and model flood susceptibility using remote sensing data using Frequency Ratio, Shannon's Entropy and Analytic Hierarchy Process.
- b) Performance evaluation of the applied models using Area Under Curve method for flood susceptibility mapping.

MATERIALS AND METHODS

The aim of flood susceptibility mapping is to identify regions that are at risk of flooding and to provide information that can be used to develop strategies for managing and mitigating the impact of floods. Flood susceptibility maps can be used for informed land-use planning decisions, including zoning, building codes, and infrastructure development.

2.1 Study Area

Khairpur District is in the northern part of province of Sindh and has spatial extent between 26° 09' and 27° 42' North latitudes and 68° 10' and 70° 10' East longitudes with an area of about 15,910 Km². Despite being a part of the Thar Desert, the land is irrigated by the River Indus, Rohri and Mir Wah canal, the main water channels passing through the district. Due to availability of the largest irrigation system, district Khairpur heavily depends upon the agriculture with wheat, cotton, dates, and sugarcane as major agriculture produce. Not only that the district Khairpur is surrounded by the irrigation network, but it also has an abundance of rainfall averaging about 87.6 mm in the monsoon season, it is also very much likely a flood prone area. In the 2010 and 2020 floods, it was one of the severely damaged areas in the Sindh province causing exponential damages.

2.2 Datasets

Flood modeling requires a mix of attribute and geo spatial data collected from different sources including ground/field survey. The details of datasets used to achieve the objectives are given below and are summarized in Table 2.1.

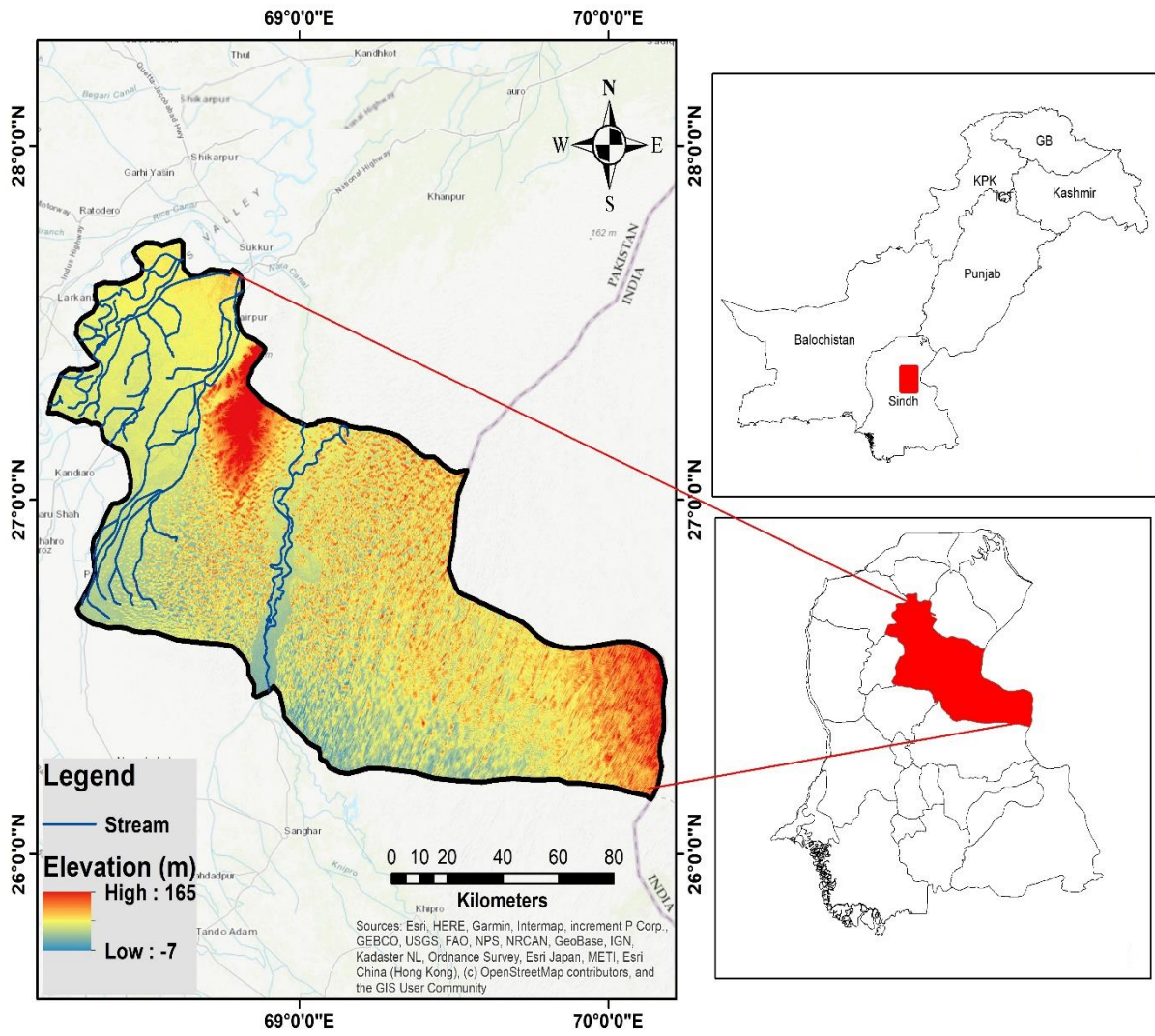


Figure 2.1. Map of study area map of district Khairpur Sindh.

Table 2.1. Summary of the data used.

Data	Source	Specification
Satellite Imagery Landsat-9	USGS	30 meters Spatial Resolution
SRTM DEM	USGS	30 meters Spatial Resolution
Precipitation	Pakistan Meteorological Department (PMD)	Millimeter Average annual
River Network	DIVA-GIS https://www.diva-gis.org/gdata	N/A
Geology Data	USGS https://certmapper.cr.usgs.gov/data/apps/world-maps/	Resolution 329*329 meter
Soil Data	FAO SOILS PORTAL https://www.fao.org/soils-portal/data-hub/soil-maps-and-databases/faunesco	Resolution 250*250 meter Depth: 30cm

2.3 Landsat Data

Landsat series has been providing continuous collection of moderate resolution multispectral data of the Earth's surface for over 40 years (USGS, 2014). The consistency of Landsat mission in provision of the free satellite imagery on a global scale makes it valuable, suitable, and economic source for mapping global changes and managing world's natural resources (Chander et al, 2009). Landsat updated its archive and now Level 1 Collection-2 Surface reflectance product is available for free of cost and on demand download. Landsat 8 has Operational Land Manager (OLI), Landsat Surface Reflectance Code (LaSRC) is used. LaSRC uses coastal aerosol band. <https://espa.cr.usgs.gov/>.

Landsat 9 continuous the Landsat program's critical role of repeating global observations for monitoring, understanding, and managing Earth's natural resources. Landsat 9 carries the Operational Land Imager 2 (OLI-2), and the Thermal Infrared Sensor 2 (TIRS-2). <https://www.usgs.gov/landsat-missions/landsat-9>. For this study, Landsat 9 satellite images of 30 meters spatial resolution were used for land use and land cover mapping. NDVI and NDWI indices were also calculated using said data.

2.4 Digital Elevation Model

Flood modeling requires the digital representation of landscape. Digital Elevation Models (DEMs) are important for flood modeling because they provide information about the topography and elevation of the land surface, a critical factor in determining how water will flow and where it will accumulate during a flood event. For this purpose, 30 meters of SRTM DEM was used for calculating Topographic Wetness Index, Slope, Curvature and Elevation map.

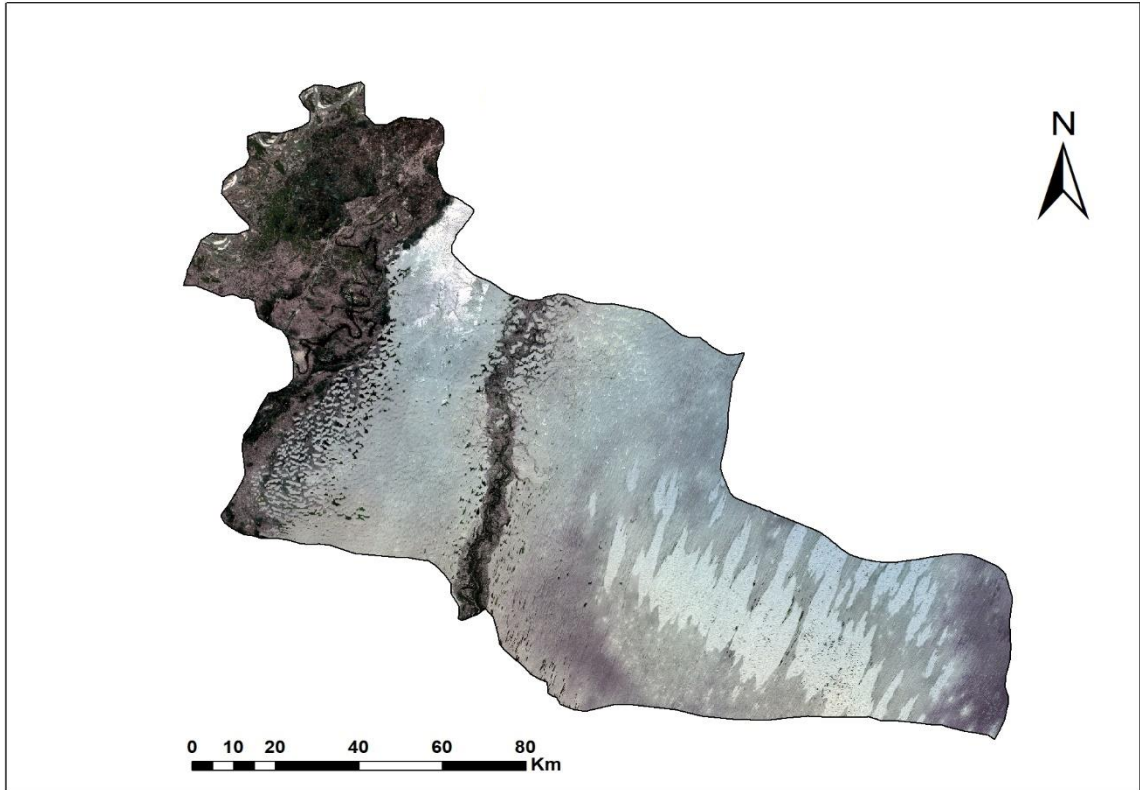


Figure 2.3. Landsat 9 image of October 2022.

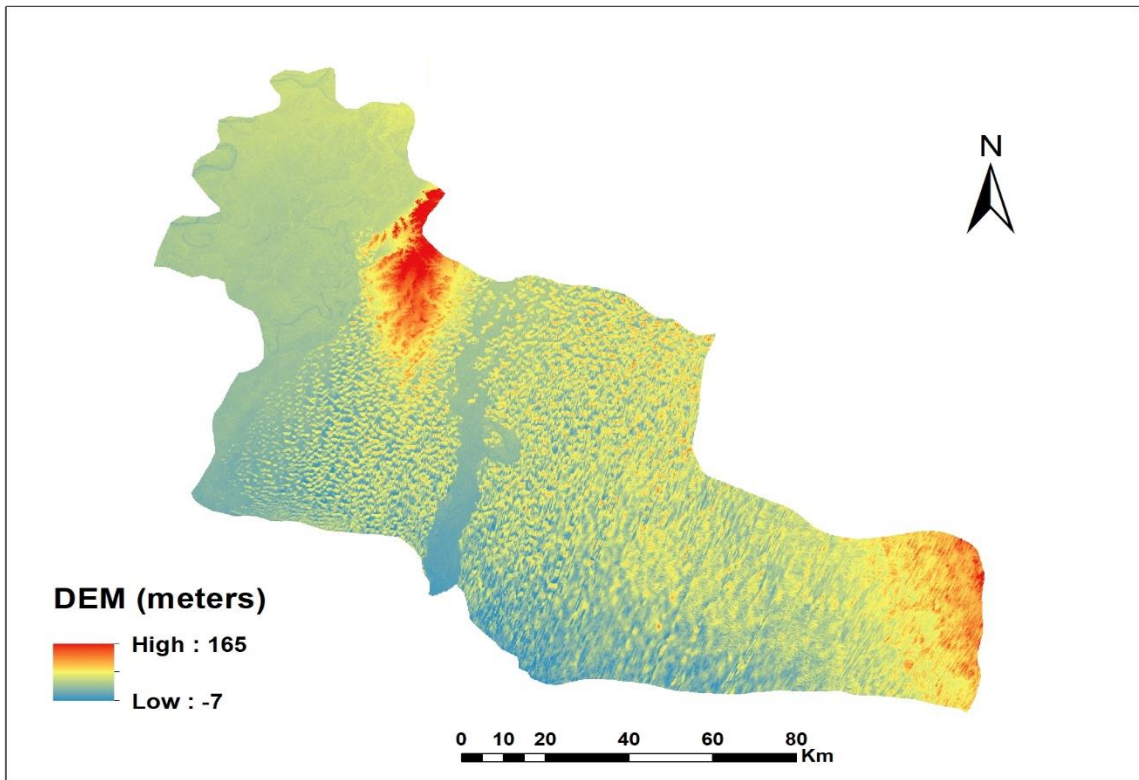


Figure 2.2. Shuttle radar topography mission 30m digital elevation model of study area.

2.5 Meteorological Data

The meteorological data were acquired from the Pakistan Meteorological Department (PMD). The assessment of data indicated that no weather station was within the premises of the study area, so all the adjacent stations were used in making the precipitation map. The lowest mean average rainfall recorded was 0.6 mm and similarly the highest was 30.1 mm. The details of ground stations used in the study are given in Table 2.2.

2.6 River Network

River network data are crucial for flood modeling because it provides information about the river channels, the direction of water flow, the shape of the river channels, and the elevation of the surrounding terrain. This information is necessary for predicting the extent and severity of flooding in each area. River/Stream network data can also be used for identifying regions that are prone to flooding, which can help for disaster preparedness and planning process. By analyzing the river network data, one can identify areas where flooding is likely to occur and develop strategies to mitigate the impacts, such as building flood protected structures, improving drainage systems, or relocating homes and businesses out of flood-prone areas. The data were obtained from the third-party source DIVAGIS (<https://www.diva-gis.org/gdata>). The platform is considered authentic and also used worldwide.

2.7 Geology data

Geology data are important for flood modeling because it provides information about the physical characteristics of the ground surface, the underlying geologic formations, and the potential pathways for water movement. By incorporating geology data into flood models, one can better understand the behavior of water during floods and develop more accurate predictions of flood susceptible areas. Lithological units with greater permeability facilitate faster infiltration, while the presence of an impermeable layer intensifies surface runoff and

causes flooding. The infiltration rate and the permeability of rocks are significantly correlated (Msabi and Makonyo, 2020). The data were downloaded from the USGS website.

2.8 Soil data

Soil data are important for flood modeling because it plays a critical role in determining how water moves through the ground and interacts with the surface. Flood modeling typically involves simulating the movement of water across a landscape, which requires an understanding of how the soil absorbs, stores, and releases water. The different types of soil in a region may have a significant impact on the likelihood of flooding, and each type of soil has a unique permeability that affects how much water can be trapped in the soil particles (Msabi and Makonyo, 2020). Soils with a high percentage of sand tend to have higher infiltration rates and lower water holding capacities, which means they can absorb and store less water before becoming saturated and generating runoff. In contrast, soil containing a high percentage of clay tend to have lower infiltration rates and higher water holding capacities, which means they can absorb and store more water before generating runoff. For this purpose, Soil data were obtained from the Food and Agriculture Organization Soils Portal.

2.9 Flood Inventory

A flood inventory is crucial for mathematical modelling process and the validation of the results. Information on the flood's location, area, etc. are included in flood inventories. Depending on the needs of the research, a flood inventory might range from simple to sophisticated. It is created based on past research, Google Earth, flood peak imagery and field survey (Panchal and Shirivastava, 2021). Flood inventory is essential in flood susceptibility mapping as it provides critical historical data that enables the identification of flood prone areas, validates flood models, supports risk assessment and management, and facilitates effective emergency response planning. Over 125 flood events are included in the

Table 2.2. Meteorological Ground Stations information.

Sr. No	Station Name	Time Period	Latitude (dd)	Longitude (dd)	Source
1	Chorr	2000-2022	25.3389	69.1303	PMD
2	Nawabshah	2000-2022	26.0884	68.3094	PMD
3	Padidan	2000-2022	26.6893	68.0595	PMD
4	Rohri	2000-2022	27.5756	68.8328	PMD

Table 2.3. Brief description of all the land use landcover types.

Sr. No	LULC	Description
1	Built-up	All the settlements.
2	Water	Water bodies of all kinds (rivers, canals, and lakes).
3	Vegetation	A general class that consists of shrub's, grassland, and agriculture area.
4	Barren land	A general class that consists of bare areas and desert.

inventory of floods in the study site. Polygons are used to show the flood extents. Figure 2.5 represents the flood inventory map.

2.10 Methodology

The study followed a systematic methodology (Figure 2.4). Moreover, this section also covers all the processing steps that were performed to obtain the final results.

2.10.1 Geospatial layers for flood susceptibility mapping

As per the methodology flow diagram the datasets have been utilized to generate numerous thematic maps in the ESRI ArcMap software. Contributing topographical parameters such as Curvature, Elevation, Topographic Wetness Index, and Slope were obtained from SRTM-DEM whereas, NDVI, NDWI, LULC was derived from Landsat 9 images. These thematic layers were then transformed to a spatial resolution of 30 m to “WGS 1984 UTM Zone 42N” coordinate system because the pixel size and coordinate system must be same of all causative factors to run the models (FR, SE, AHP). All the causative factors were prepared in ArcGIS software. Finally, Frequency Ratio, Shannon’s Entropy and Analytical Hierarchy Process were applied in decision making to produce flood susceptibility maps of the study area.

2.10.2 Flood causative factors

The delineation of flood-prone areas is a crucial concern for water resources and land use planning and management (Liuzzo et al, 2019). Several causative factors and their relationship

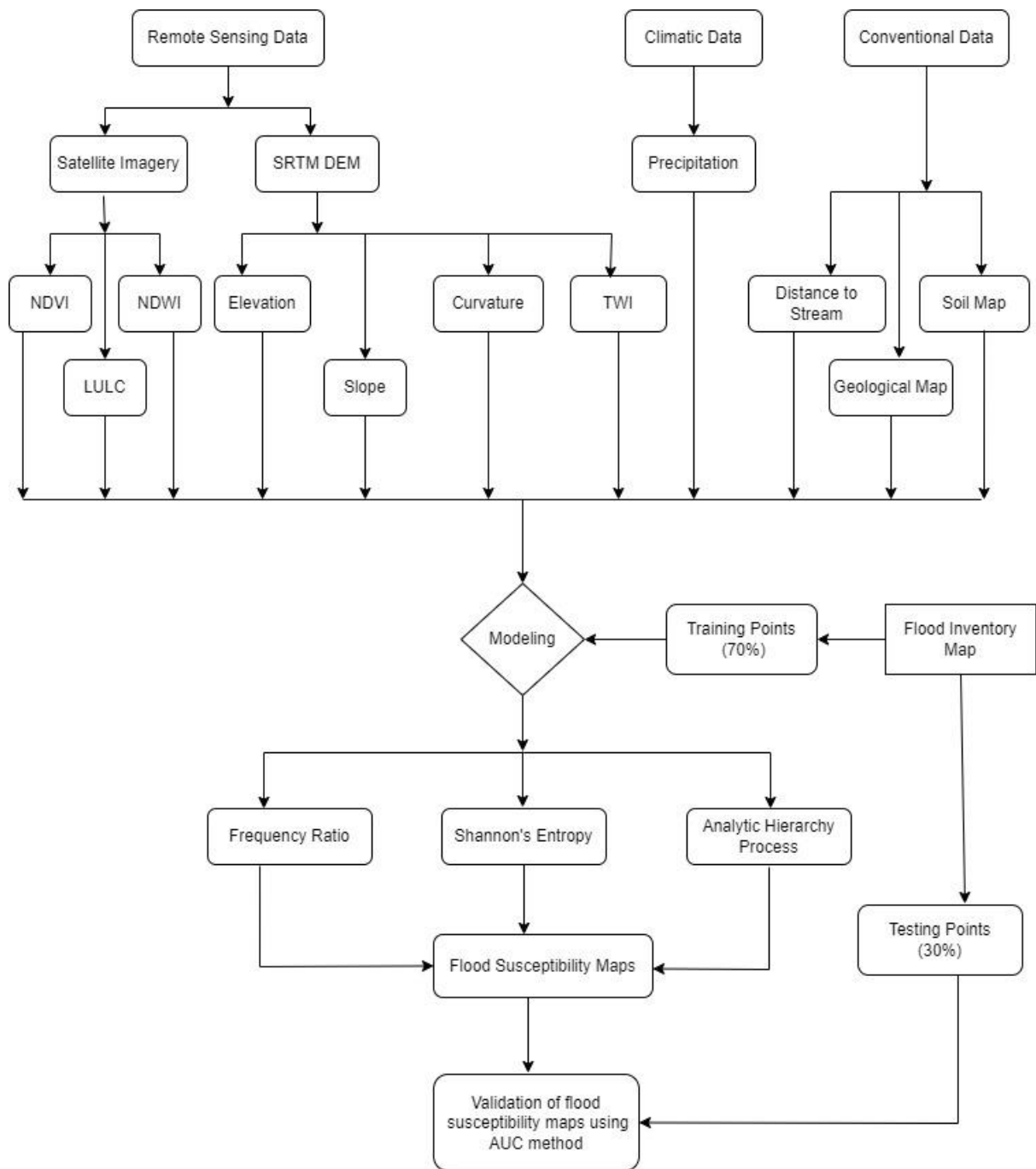


Figure 2.4. Flow chart of methodology.

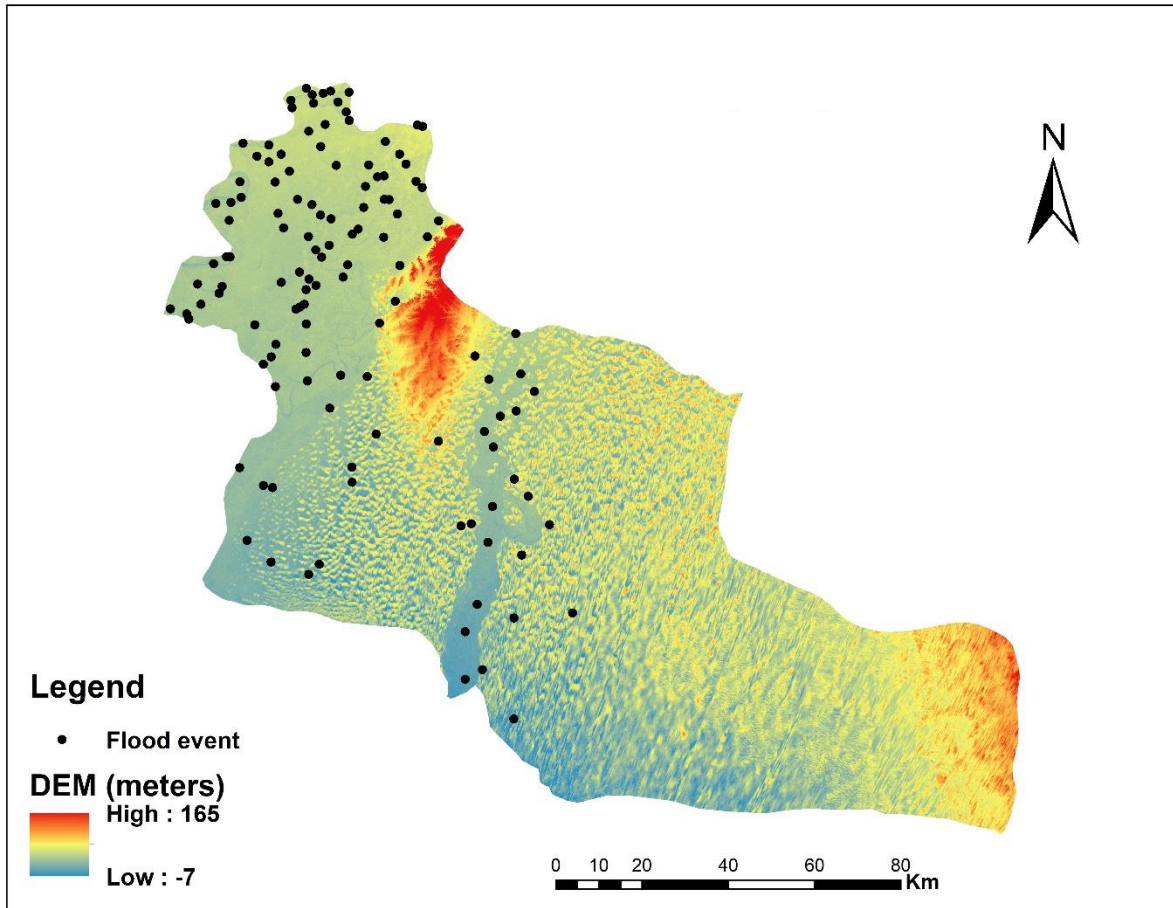


Figure 2.5. Flood inventory map.

Table 2.4. Classification of area under curve range.

AUC Values	Test Quality
0.5-0.6	Unsatisfactory
0.6-0.7	Satisfactory
0.7-0.8	Good
0.8-0.9	Very good
0.9-1.0	Excellent

to floods must be looked in order to determine flood vulnerable areas (Tehrany et al, 2013). The selecting of the flood causative factors, often referred to as contributing factors/parameters to flooding across a region, is of utmost significance in impacting the accuracy of the results. However, there isn't a framework that is generally accepted for choosing the flood causative factors, even though this would imply their important significance in flood susceptibility mapping (Msabi and Makonyo, 2020).

In this study, eleven parameters that can influence floods were incorporated, which include Elevation, Slope, Curvature, Topographic Wetness Index, NDVI, NDWI, LULC, Distance to stream, Average annual rainfall, Soil, Geological map. The natural breaks classification algorithm was used to classify each flood causative factor.

2.10.3 Accuracy Assessment

It is important to have a clear and accurate record of the previous flood events to create flood susceptibility maps (Merz et al, 2007). An important part in every modelling process is accuracy assessment (Bui et al, 2011). The “Area Under Curve (AUC)” method is commonly employed in natural hazard studies because of its thorough, rational, and easily understandable validation technique (Nefeslioglu et al, 2010). The flood probability index is first arranged in descending order. Then, using cumulative 1% breaks on the x-axis, the ordered flood probability index is divided into 100 groups on the y-axis. The flood inventory is then imposed on the flood probability index. Prediction and success rates are calculated once the existence of the flood points (training and testing) in each class is assessed (Pourghasemi et al, 2012). The AUC technique generates two key outputs i.e., success rates and prediction rates. The flood training dataset is utilized to calculate the success rate, while the flood testing dataset is employed to determine the prediction rate. AUC generates a range from 0 to 1. If the AUC value is 1, the method is 100% effective. Therefore, the more accurate the method, the closer the AUC value is to one (Tehrany et al, 2018). The formula for AUC calculations is as follows.

$$\text{Overall accuracy} = \frac{TP + TN}{TP + TN + FP + FN} \quad (1)$$

In the validation and training datasets, TN and TP are true negative and true positive values respectively and these are the number of samples correctly classified as flood and no-flood class. FN and FP are false negative and false positive values which are the number of samples not accurately classified.

The effectiveness and performance of the three models Frequency Ratio, Shannon's Entropy and Analytic Hierarchy Process were assessed in this study using the AUC method.

2.11 Modelling Approach

2.11.1 Analytic Hierarchy Process (AHP)

This method has received the most attention and was used to develop a unique framework for making decisions on flood susceptibility mapping (Swain et al, 2020). It is a decision-making tool that assists in resolving complicated issues using simple criteria. The three guiding concepts of AHP are problem decomposition, comparative evaluation, and rankings. The issue/problem is divided into hierarchical criteria in AHP. Flood causative factors are compared with one another. i.e., Pair-wise comparison (Panchal and Shrivastava, 2021). The significance of the chosen flood causative factors was determined by considering expert knowledge and information from existing literature. It ranges from 7 (highest significance) to 1 (lowest significance) (Vojtek and Vojteková, 2019). (Saaty, 1980) said that the consistency of the AHP method is represented by the relation.

$$CR = \frac{CI}{RI} \quad (2)$$

$$CI = \frac{\lambda_{\max} - n}{n - 1} \quad (3)$$

In the context of the given information, CR stands for the consistency ratio, CI denotes the consistency index, RI denotes the random index, λ_{\max} corresponds to the principal eigenvalue of the matrix, and n signifies the total number of parameters within the matrix. The CR is computed using RI values, which are dependent on the number of parameters present in the comparison matrix (Saaty, 1980). In this study, eleven parameters were utilized, resulting in an RI value of 1.51. A CR value below 0.10 is considered acceptable and indicates good accuracy for the pairwise comparison matrix. However, if the CR value exceeds 0.10, it signifies inconsistency in the comparison matrix, necessitating adjustments to be made (Saaty, 1977). The flood susceptibility (FS) is determined by considering the weights (w_i) assigned to each parameter (i) and the corresponding flood susceptibility classes (x_i) for each factor.

$$FS = \sum W_i X_i \quad (4)$$

2.11.2 Frequency Ratio

The FR is a productive bivariate statistical analysis technique used in studies of natural hazards, such as landslide susceptibility mapping (Chen et al, 2021), flood susceptibility mapping (Jothibas and Anbazhagan, 2016), ground water potential zone mapping (Manap et al, 2014), soil erosion mapping (Khosrokhani and Pradhan, 2014) and mineral potential mapping (Yusoff et al, 2015). Its widespread use is due to its quick and easy computation method (Choi et al, 2011). FR serves as a straightforward and convenient geospatial assessment tool to comprehend the probabilistic connection between dependent and independent variables, encompassing multi-classified maps (Rahmati et al, 2015).

The FR, a measurement, is the ratio of an event's likelihood of occurring to its probability of not occurring. Flood occurrence and the causative parameter are strongly

correlated when FR is greater than one and weakly correlated when FR is less than one. Flood parameter raster maps are categorized using the natural break approach in a GIS context to produce flood susceptibility maps. (Liuzzo et al, 2019). The equation 5 show how the FR values computed for each class of the parameter:

$$FR = \frac{A/B}{M/N} \quad (5)$$

A refers to the number of flood pixels for each class of causative factor, while B represents the total number of flood pixels within the study area. M denotes the count of pixels for each class of the causative factor, and N stands for the total number of pixels in the study area.

Once the FR values are computed for each class of causative factors, the flood susceptibility index (FSI) is evaluated for each pixel within the study area using the following equation:

$$FSI = \sum_{i=1}^n FR_i \quad (6)$$

where FR_i is the FR value for the class of factor i and n is the total number of causative factors.

2.11.3 Shannon's Entropy

Entropy serves as a metric to assess disparities between causes and outcomes or decisions across various debated subjects (Khosravi et al, 2016). The entropy index quantifies abnormality, unstable behavior, and uncertainty within each system, reflecting the extent of irregularity between causes and outcomes in different issues. The Shannon's entropy information model was derived by enhancing the Boltzmann principle, which establishes a connection between quantity and entropy (Islam et al, 2021). The equation to calculate the

information coefficient V_j , which represents the weight value for the causative factors, is provided by the approach presented by (Naghibi et al, 2015).

$$E_{ij} = \frac{FR}{\sum_{j=1}^{M_j} FR} \quad (7)$$

$$H_j = - \sum_{i=1}^{M_j} E_{ij} \log_2 E_{ij}, j = 1, \dots, n \quad (8)$$

$$H_{jmax} = \log_2 M_j \quad (9)$$

$$I_j = \frac{H_{jmax} - H_j}{H_{jmax}}, I = \quad (10)$$

$$V_j = I_j \quad (11)$$

In the given context, FR represents the frequency ratio, E_{ij} stands for the probability density, H_j and H_{jmax} denote entropy values, I_j refers to the information coefficient, M_j represents the number of classes, and V_j is the achieved weight value for the parameters.

RESULTS AND DISCUSSION

3.1 Flood Causative Factors

Hydro-geomorphological and geological data can be used in flood susceptibility modelling in line with the physiological features of a specific place. There are no set guidelines or procedures for determining how many floods causative factors are sufficient and what kinds of factors should be considered (Islam et al, 2021). Several causative factors and their relationship to floods must be investigated to determine flood vulnerable areas (Tehrany et al, 2013).

The most important and relevant flood causative factors from recent studies have been incorporated into this study for flood susceptibility mapping. Eleven flood causative factors were selected, and thematic maps were prepared. Their influence on floods is explained below in detail.

3.1.1 Elevation

Elevation maps play a crucial role in flood susceptibility mapping due to their ability to provide valuable information about the topography and terrain of an area. The surface runoff always flows swiftly from areas of high to low elevations, respectively. Low land areas flood more easily and faster than highly elevated areas (Msabi and Makonyo, 2021). The elevation map was prepared by utilizing 30 meters SRTM DEM for the study area and divided into five classes based on elevation: (1) 0-23 m, (2) 23-68 m, (3) 68-111 m, (4) 111-152 m, (5) 152-180 m as shown in Figure 3.1.

3.1.2 Slope

Surface runoff and water accumulation process in any geomorphic setting relies upon its surface slope appropriation. Water velocity and flood power are commonly constrained by

the topographic slope (Das, 2020). The slope map was prepared by utilizing 30 meters SRTM DEM for the study area and divided into five classes based on slope: (1) 0-3.9 degree, (2) 3.9-7.8 degree (3) 7.8-12.9 degree, (4) 12.9-20.7 degree, (5) 20.7-99.9 degree as shown in Figure 3.2.

3.1.3 Curvature

Curvature maps are important in flood susceptibility mapping due to their ability to provide insights into the shape and characteristics of the terrain. Curvature maps help to identify concave, convex and flat regions on the landscape. The curvature map was prepared by utilizing 30 meters SRTM DEM for the study area and divided into five classes: (1) -152 - -8004, (2) -8004 - -3024, (3) -3024 - 7115, (4) 7115-5692, (5) 5692-1451 as shown in Figure 3.3.

3.1.4 Topographic Wetness Index

TWI as an index can predict areas susceptible to wetted land surfaces and areas that have strong potential to produce overland flow and this parameter as a physical depiction of areas that are highly prone to flood inundation (Das, 2020). The TWI map was prepared by utilizing 30 meters SRTM DEM for the study area and divided into five classes: (1) -8.1 - -4.1, (2) -4.1 - -1.6 (3) -1.6-0.9, (4) 0.9-4.0, (5) 4.0-13.8 degree as shown in Figure 3.4.

3.1.5 Normalized Difference Vegetation Index

NDVI is an index representing the vegetation density over an area, and it is one of the factors used for determining flood susceptibility. Higher vegetation density decreases the speed of the runoff and flood inundation (Tehrany et al, 2018). The NDVI map was prepared by Landsat 9 imagery for the study area and divided into five classes: (1) -0.1 - 0, (2) 0- 0.06 (3) 0.06-0.12, (4) 0.12-0.2, (5) 0.2-0.4 as shown in Figure 3.5.

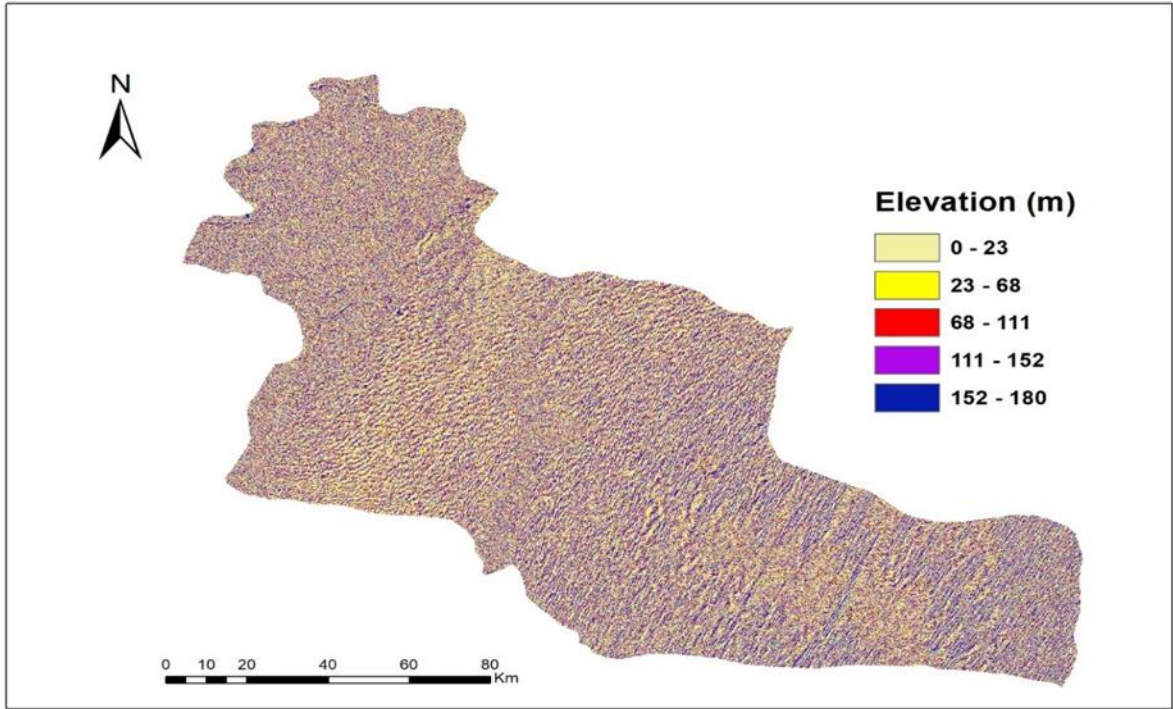


Figure 3.1. Elevation map of the study area.

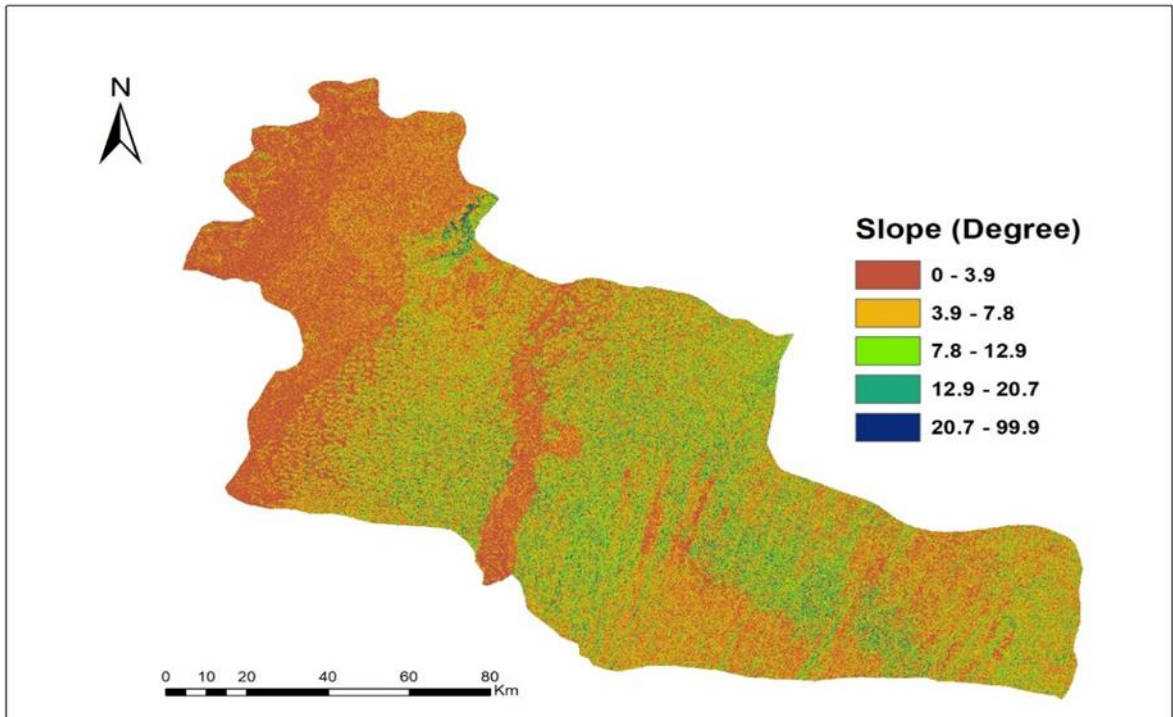


Figure 3.2. Slope map of the study area.

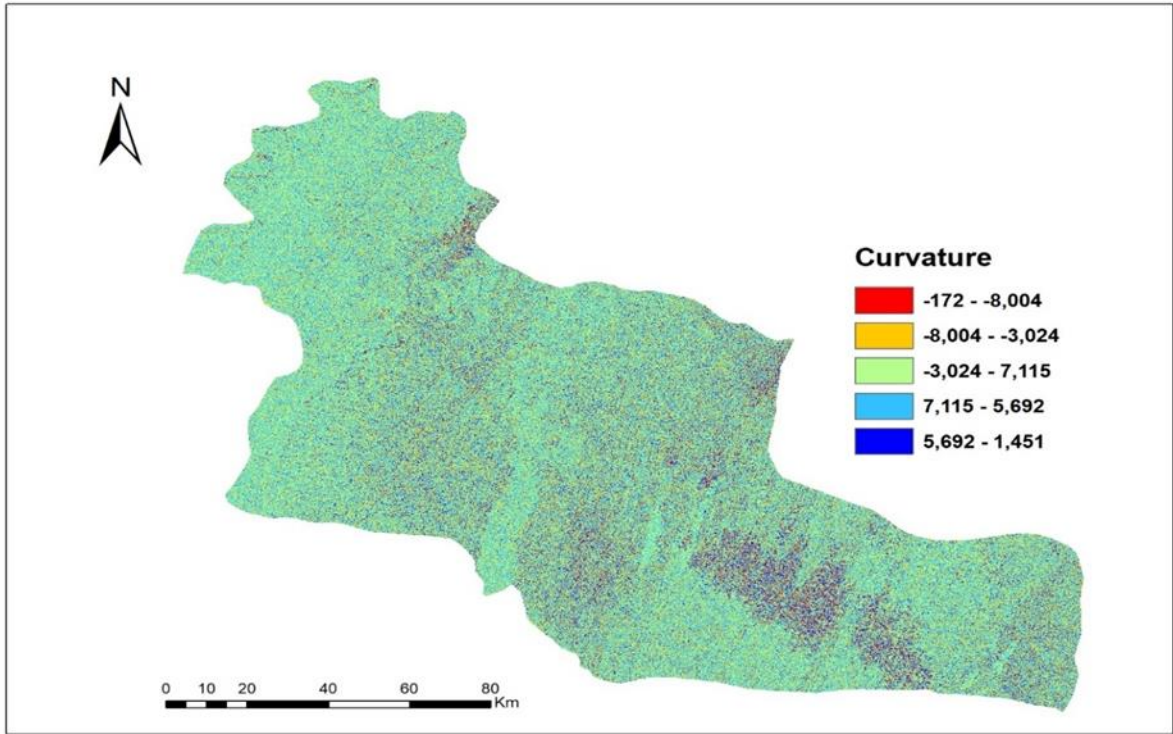


Figure 3.3. Curvature map of the study area.

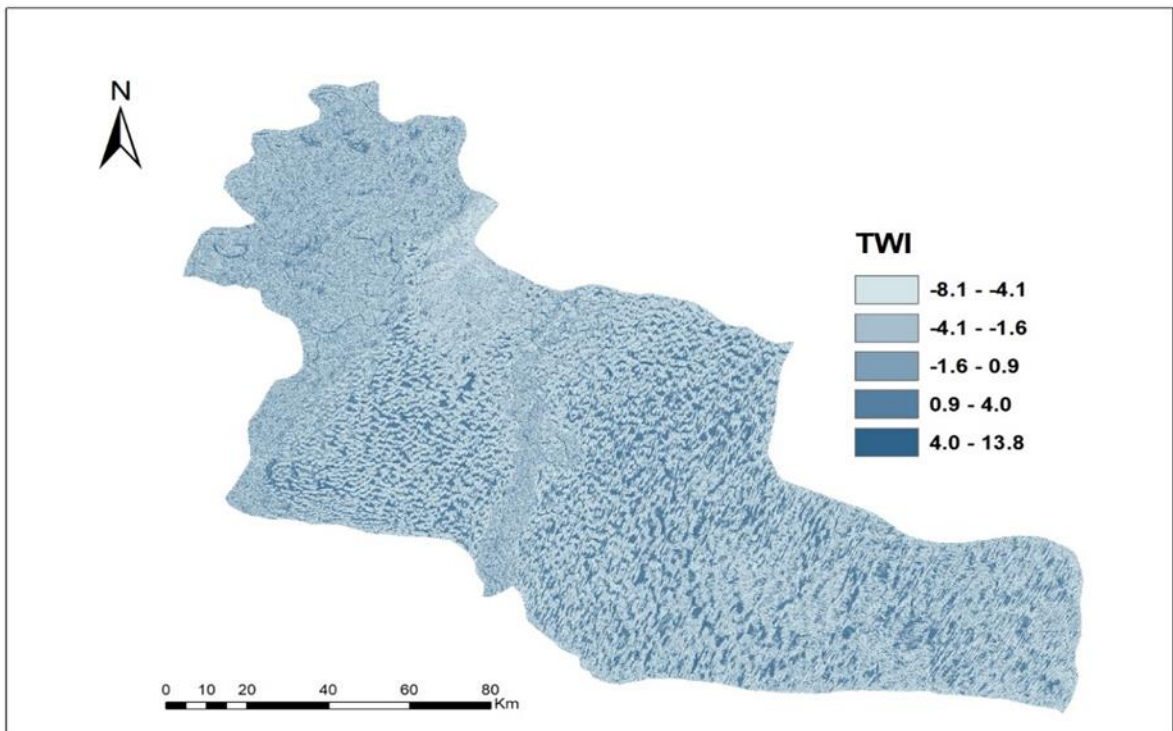


Figure 3.4. Topographic wetness index map of the study area.

3.1.6 Normalized Difference Water Index

NDWI is another important index used in flood susceptibility mapping. It focuses on the presence and distribution of water bodies, such as rivers, lakes, and wetlands, and can provide valuable information for assessing flood susceptibility. The NDWI map was prepared by Landsat 9 imagery for the study area and divided into five classes: (1) -0.4 - -0.1, (2) -0.1 - -0.13 (3) -0.13 - -0.10, (4) 0.10 - -0.03, (5) -0.03 - 0.16 as shown in Figure 3.6.

3.1.7 Land Use Land Cover

The LULC plays a vital role in identifying zones that show high susceptibility to flooding. The occurrence of flooding in the area can be greatly influenced by the surface cover or land-use patterns and change of an area over time (Msabi and Makonyo, 2021). LULC map is derived from Landsat 9 imagery, supervised classification was done and a total of four LULC classes were generated: (1) Built up, (2) Water, (iii) Vegetation, (iv) Barren land as shown in Figure 3.7.

3.1.8 Distance to stream

Areas that are close to streams/rivers have a higher probability of flood inundation than areas located far away from the rivers since surplus water from the rivers initially reaches alongside stream/riverbanks and adjoining lowland areas. This is because as the distance increases, the slope and elevation become higher (Negese et al, 2022). The distance to stream map was prepared in Arc Map and divided into five classes based on distance: (1) 0-15.8 km, (2) 15.8-39.7 km (3) 39.7-66.1 km, (4) 66.1-96.1 km, (5) 96.1-129.6 km as shown in Figure 3.8.

3.1.9 Average Annual Rainfall

Rainfall is the most crucial triggering factor for the occurrence of floods because flood inundation is due to a huge volume of runoff flows because of excessive heavy rainfall or

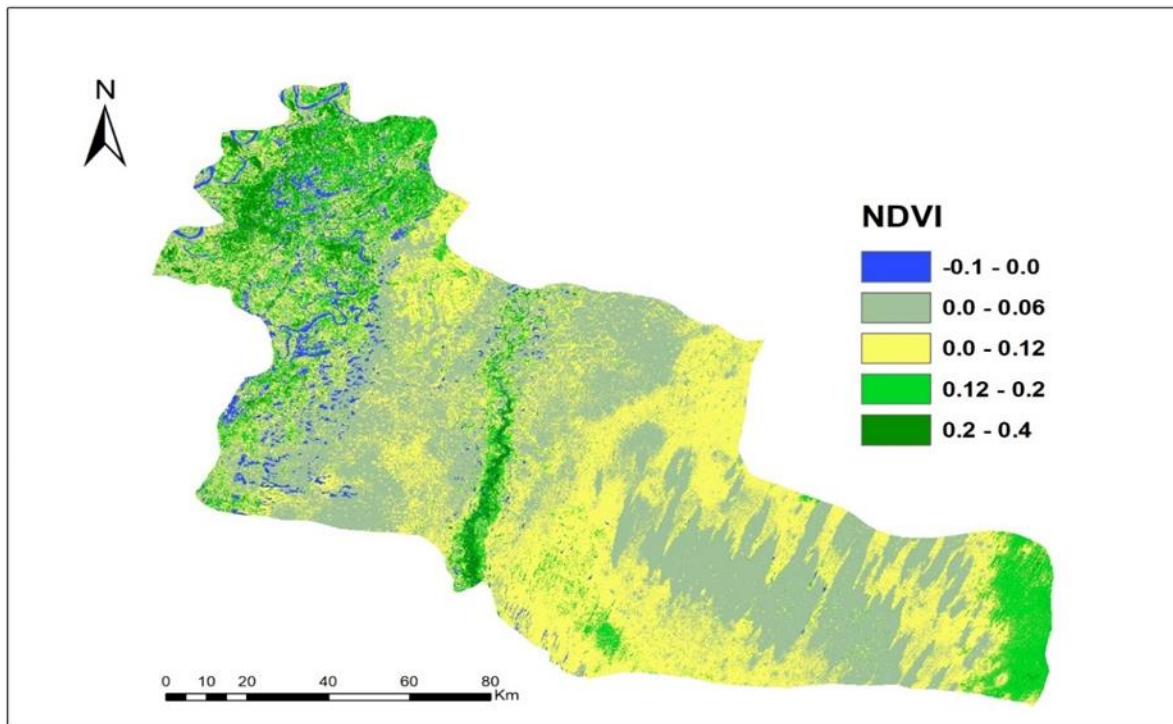


Figure 3.5. Normalized difference vegetation index of the study area.

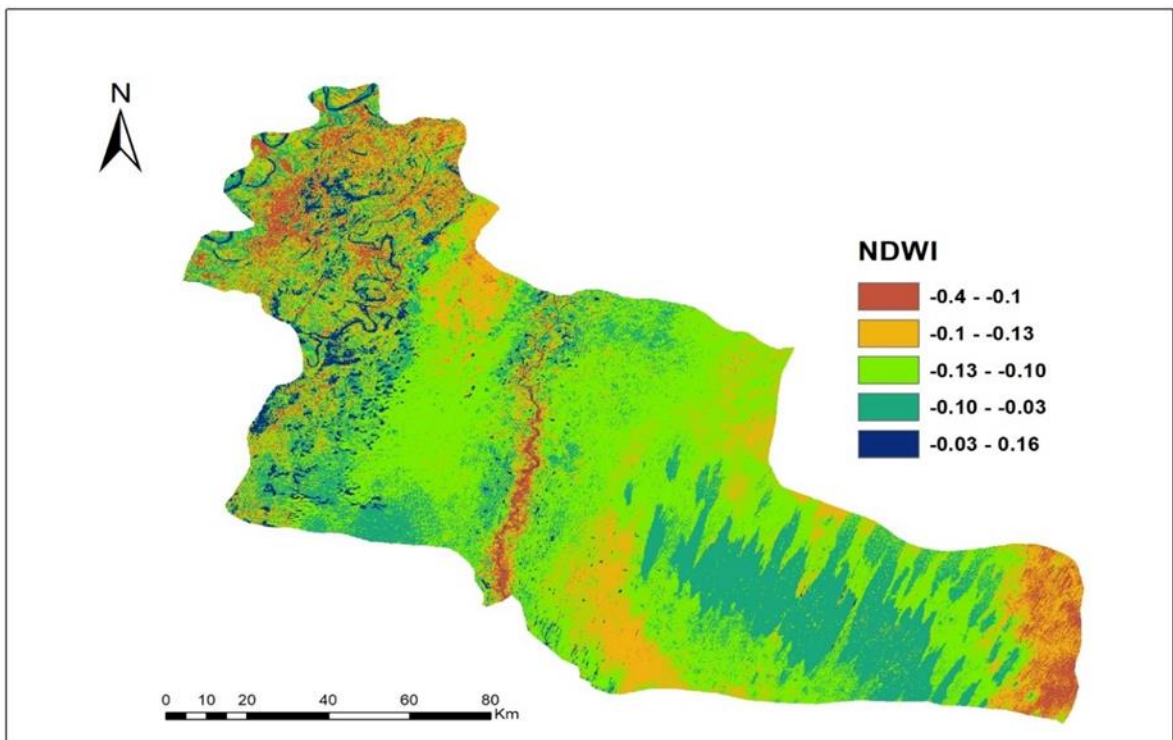


Figure 3.6. Normalized difference water index of the study area.

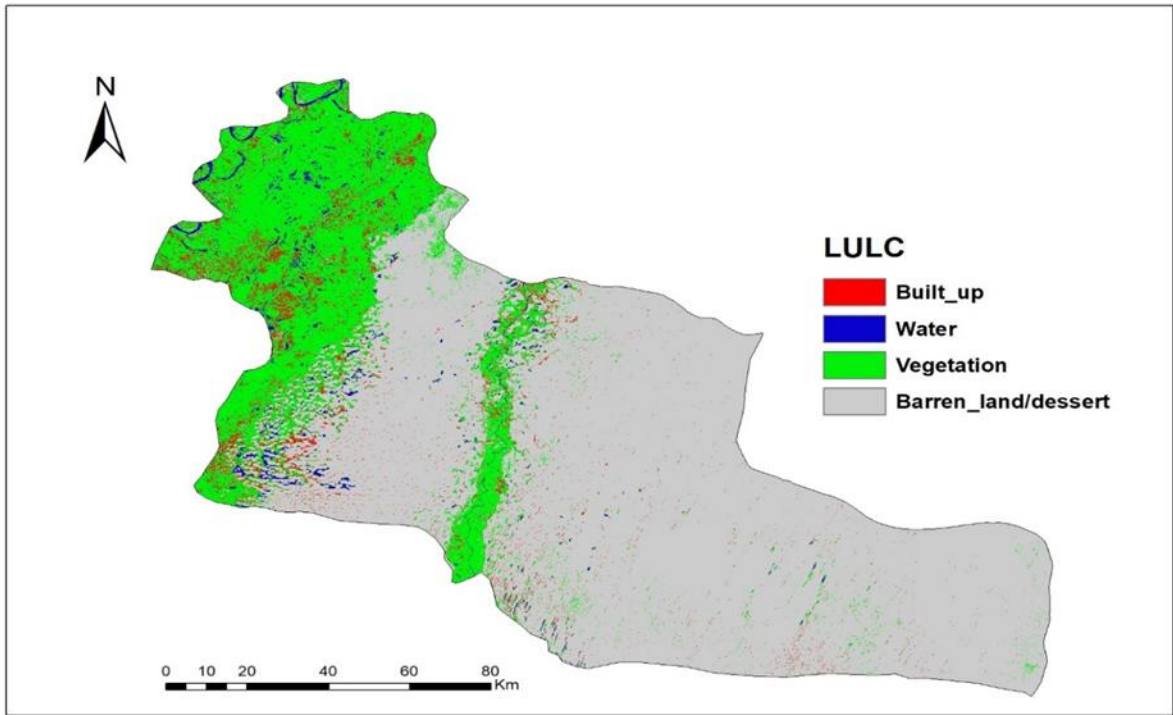


Figure 3.7. Land Use Land Cover of the study area.

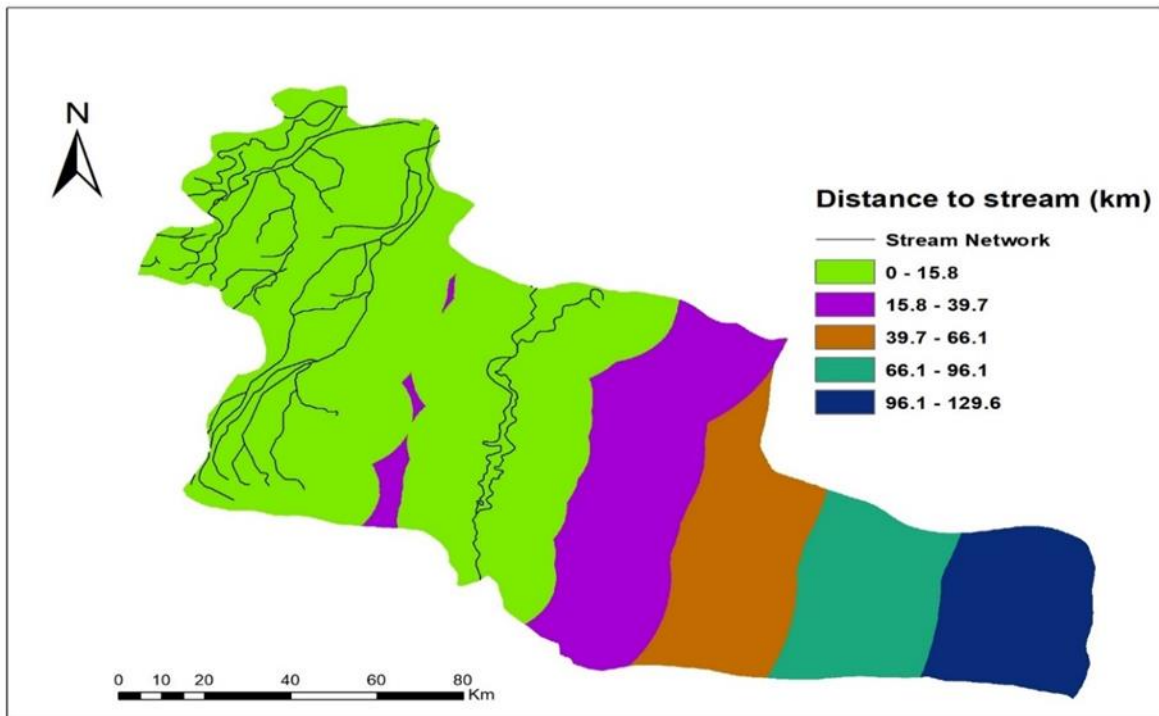


Figure 3.8. Distance to stream map of the study area.

prolonged rainfall (Nagese et al, 2022). The rainfall data were acquired from the Pakistan Meteorological Department (PMD). The lowest mean average rainfall recorded was 0.6 mm and similarly the highest was 30.1 mm. The rainfall map was classified into five classes: (1) 0.6-5.7 mm, (2) 5.7-11.2 mm, (3) 11.2-17.7 mm, (4) 17.7-23.8 mm, (5) 23.8-30.1 mm as shown in figure 3.9.

3.1.10 Soil

Soil texture has great control over the infiltration mechanism. In general, soil composed of a large proportion of fine particles (clay and silt) has higher runoff generation as water can't infiltrate through the fine pores. By contrast, a large proportion of coarse particles (sand) increase infiltration and leads to reduced runoff. (Das, 2020). Major soil textures in the study area are (1) Loam, (2) loamy sand (3) Clay loam, (iv) Sandy loam.

3.1.11 Geology

Geology plays a dominant role in flood susceptibility studies because of different susceptibilities of lithological units to active hydrological processes. Areas with high resistant rocks or highly permeable subsoil material have low drainage density and it influences the way water flows and interacts with the landscape (Rahmati et al, 2015).

3.2 Frequency Ratio Model

The FR is a bivariate statistical analysis method used in flood modeling and defined as the ratio of the probability of occurrence to the probability of non-occurrence for a given event. FR is used to evaluate the influence of the classes of each flood causative factor on flood occurrence (Liuzzo et al, 2019). FR value for each class of flood causative factor was calculated by dividing the flood occurrence ratio with the total area ratio, as shown in Table 3.1. A higher FR weight indicates a stronger correlation between a class and the likelihood of flooding, which translates to a higher likelihood of flooding in that class.

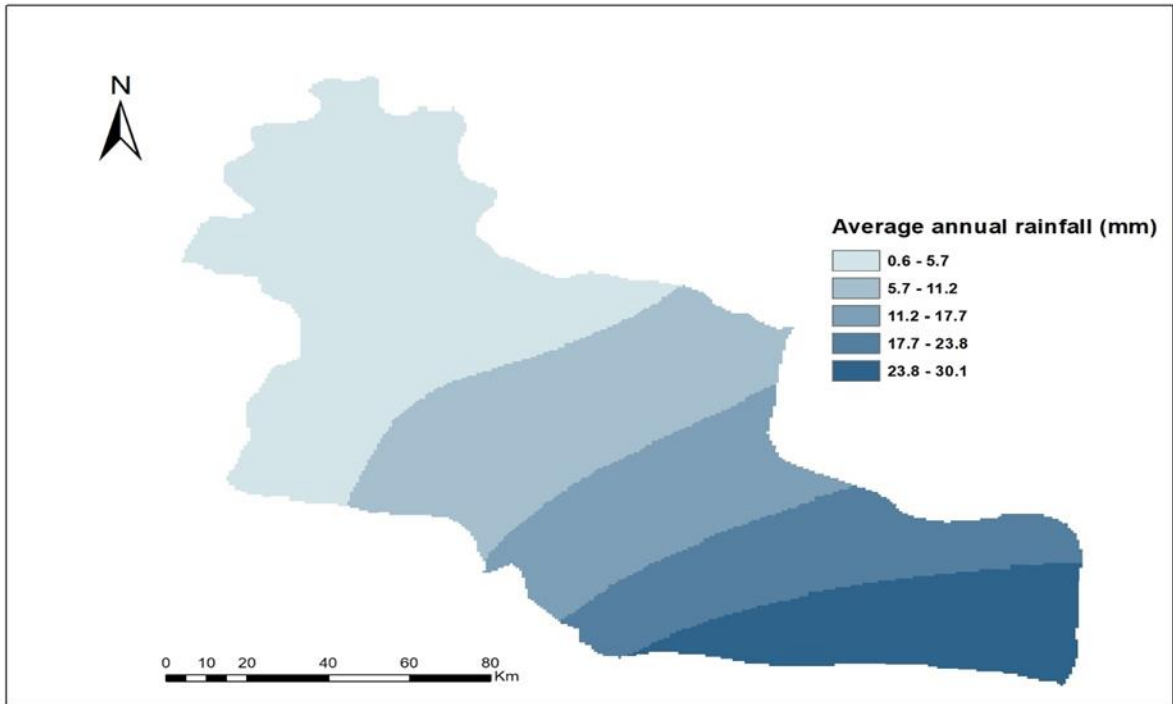


Figure 3.9. Average annual rainfall map of the study area.

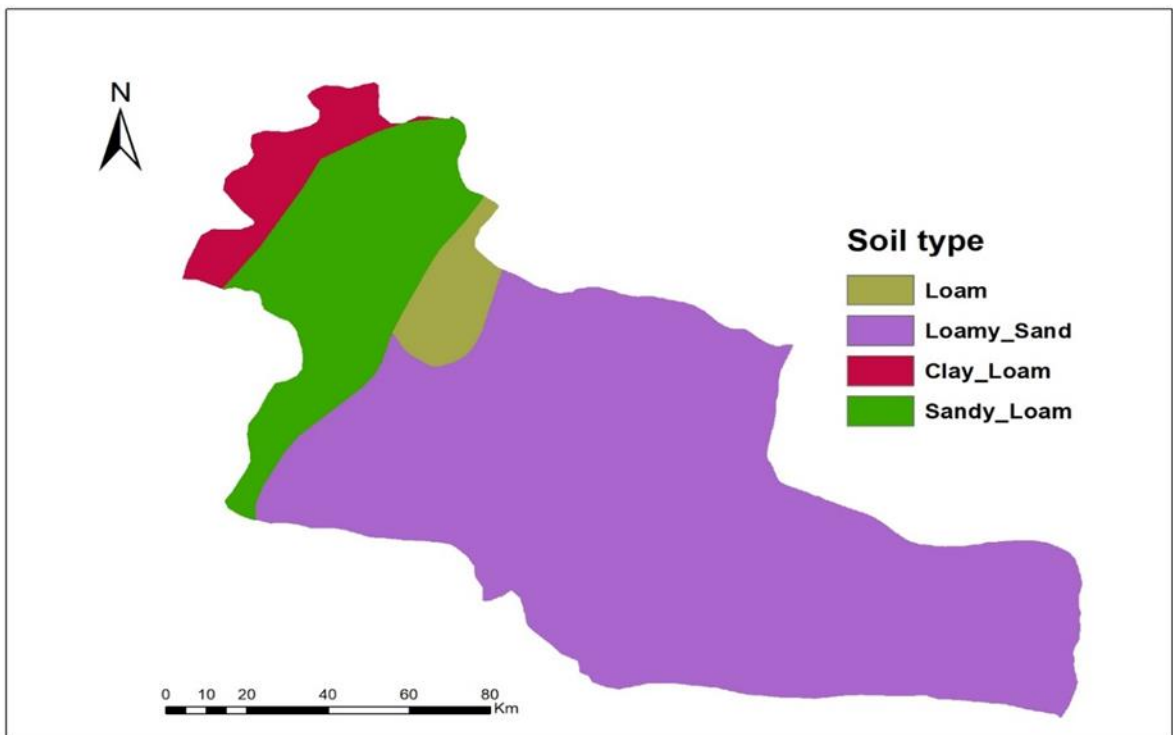


Figure 3.10. Soil texture map of the study area.

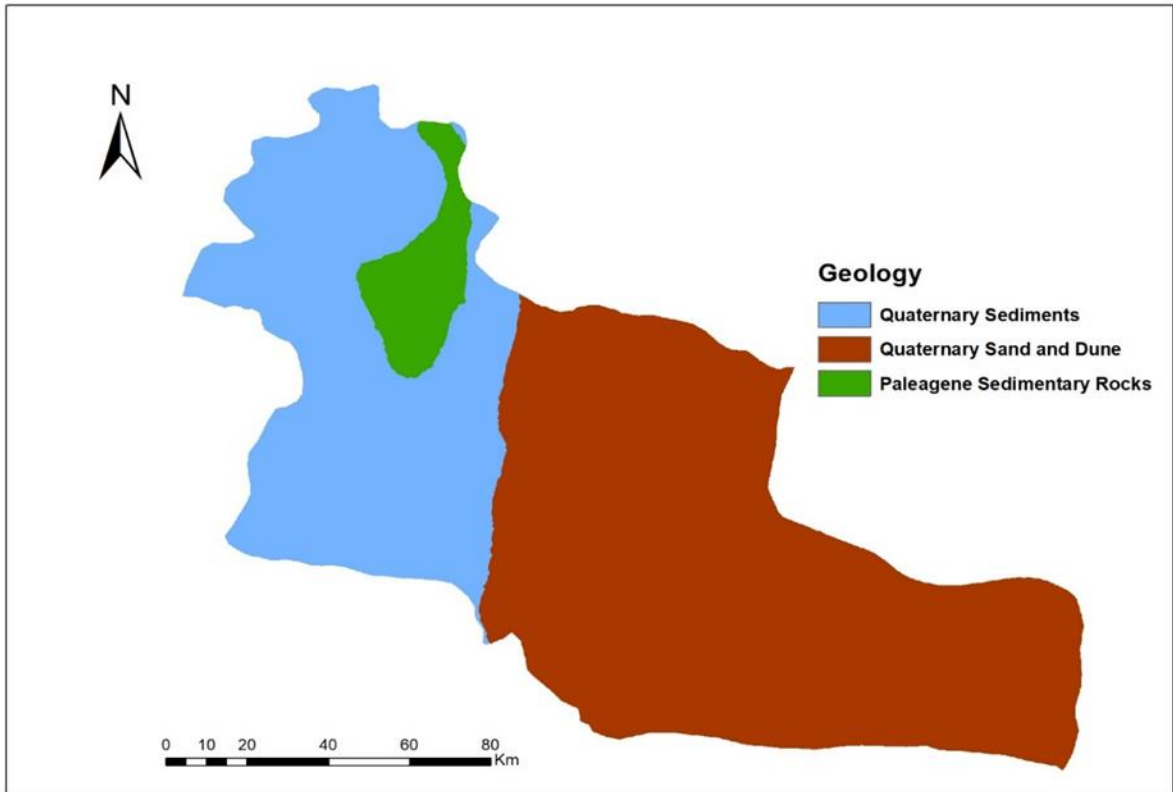


Figure 3.11. Geological map of the study area.

Table 3.1 shows that Rainfall, soil, and distance to stream were the most contributing and elevation contributed the least because the study area is mostly plain.

The largest FR value is seen at slopes less than 3.9 degrees, suggesting that the risk of flooding is greatest on these moderate slopes. The FR values for the other slope classes, however, are noticeably lower. It is clear from Table 3.1, that the flood risks associated with various soil types, clay loam regions are the most vulnerable. Soils with a high percentage of sand tend to have higher infiltration rates and lower water holding capacities, which means they can absorb and store less water before becoming saturated and generating runoff. In contrast, soil with a high percentage of clay content tends to have lower infiltration rates and higher water holding capacities, which means they can generate immediate runoff. The findings of the flood susceptibility study show a significant correlation between LULC and the likelihood of flooding. Areas around water bodies have the greatest flood risk ratings. Furthermore, flood occurrences and the hydrological component TWI indicate a strong association, with the third and fifth TWI classes because they are displaying the highest FR values. According to the FR values analysis for the NDWI map, areas around the streams are more prone to flooding.

The distance from a stream is a critical element that considerably influences floods (Tehrany et al, 2013). The highest FR values are found in areas that are less than 15.8 km from the stream network, with the flood risk being almost zero (or very close to it) for all other distance classes. In layman's words, the interpretation implies that the risk of flooding reduces with distance from the river.

The first class, which corresponds to rainfall less than 5.7 mm, has the greatest FR value. The risk of floods is unaltered despite an increase in rainfall. This is probably because

areas with sandy soil in the desert receive rain. However, floods are less likely to occur there since the sand's high imperviousness effectively absorbs much of the precipitation.

The “Flood Susceptibility Index (FSI)” values are calculated for each cell of the grid using the FSI equation of Frequency Ratio. The results are shown in the map in Figure 3.12. FSI ranges between 292.806 and 17059.1. Low FR values, which imply a reduced risk of floods, show a site's sensitivity to flooding. On the other hand, places where floods are more likely are associated with higher FR values. There are five main classifications based on the Flood Susceptibility Index values. Very low (292–2791), low (2791–6078), moderate (6078–9432), high (6078–12522) and very high susceptibility (12522–17059). Figure 3.12 represents the flood susceptibility map acquired using the frequency ratio model.

Figure 3.13 describes the spatial distribution of the flood susceptibility identified using Frequency Ratio Model. According to the chart 8% of the area is very high, 23% is high, 10% is moderate, 14% is low, and 45% is very low for flood susceptibility. A careful inspection indicates that the very high areas are the ones adjacent to the river Indus and similarly the high areas are the ones that contain the stream channels and zone showing very low flood susceptibility are the area of the Thar Desert.

3.3 Shannon’s Entropy Model

Entropy serves as a metric to assess disparities between causes and outcomes or decisions across various debated subjects. Entropy index is the measure of changeability, unstable behavior, and uncertainty in each system. (Khosravi et al, 2016). The FR output values are used to calculate the Shannon's Entropy Index in accordance with the approach described in the paper by (Liuzzo et al, 2019). Table 3.2 shows the results of SE model. Rainfall has the highest weight (0.163), followed by distance to stream (0.158 km), and soil (0.152), among the

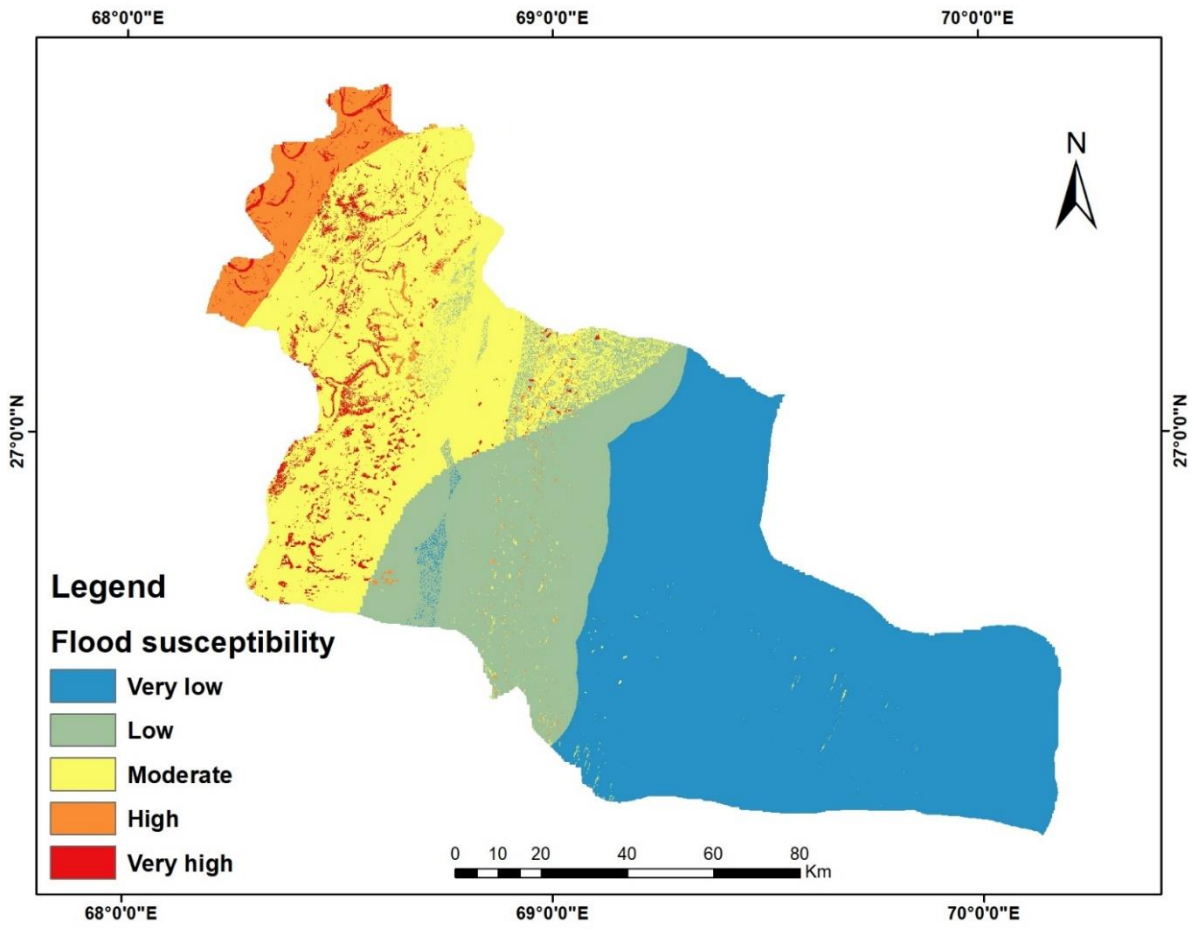


Figure 3.12. Flood susceptible zones using frequency ratio.

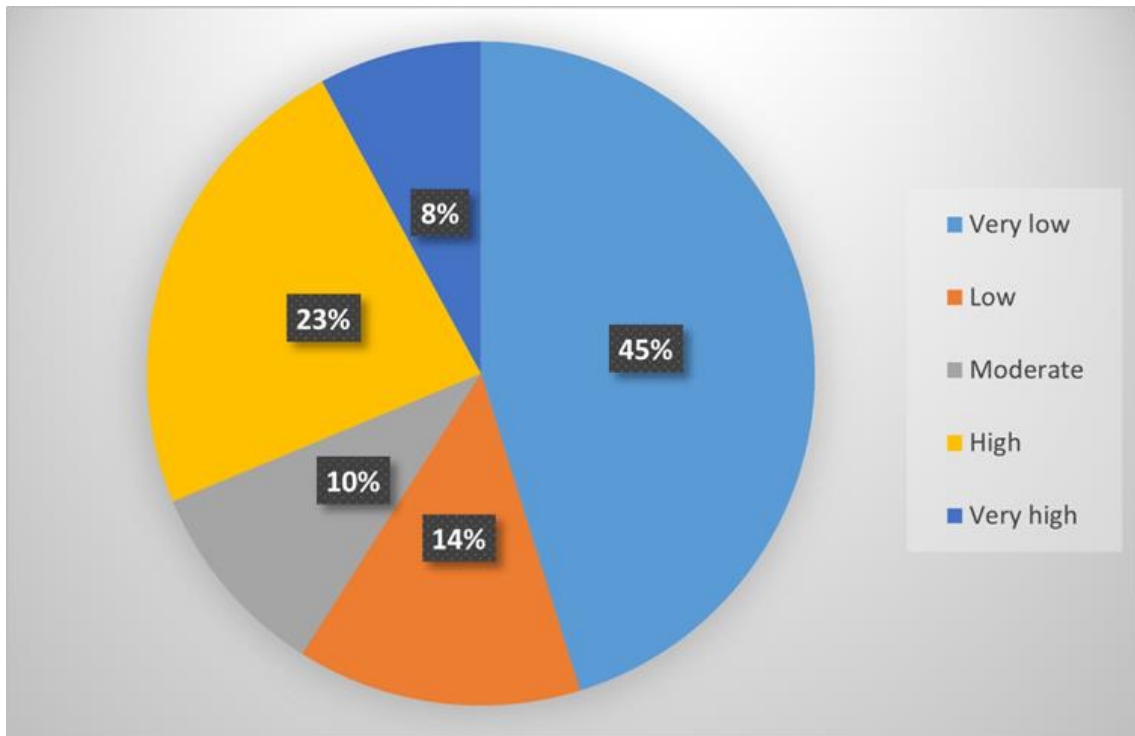


Figure 3.13. The calculated area of flood susceptibility zones.

Table 3.1. Frequency Ratio for each class of each parameter.

Parameter	Class	Class Pixels	Flood Pixels	Frequency Ratio	Prediction Ratio (FR)
Slope(Degree)	0-3.9	7552791	29210	0.0039	18.9
	3.9-7.8	5570704	8225	0.0015	
	7.8-12.9	2813628	1530	0.0005	
	12.9-20.7	1170372	288	0.0002	
	>20.7	281648	47	0.0002	
Elevation (m)	0-23	9512968	20347	0.0021	1
	23-68	1141200	2680	0.0023	
	68-111	1291277	2947	0.0023	
	111-152	1980443	4660	0.0024	
	152-180	3456505	8661	0.0025	
Rainfall (mm)	0.6-5.7	6395704	37236	0.0058	29.2
	5.7-11.2	3696680	1168	0.0003	
	11.2-17.7	2353488	662	0.0003	
	17.7-23.8	2557277	0	0.0000	
	23.8-30.1	2316184	0	0.0000	
Soil	Loam	640906	347	0.0005	28.8
	Loamy Sand	12952076	5649	0.0004	
	Clay Loam	897347	27011	0.0301	
	Sandy Loam	2916078	6296	0.0022	
LULC	Built-up	591939	3519	0.0059	24.9
	Water	281524	11575	0.0411	

	Vegetation	3963621	23122	0.0058	
	Barren Land	12573466	1088	0.0001	
Geology	Quaternary Sediments	6081808	34615	0.0057	22.5
	Quaternary Sand and Dune	10458334	3199	0.0003	
	Paleogene Sedimentary Rock	870508	1490	0.0017	
TWI	"-8.1 - -4.1"	6968666	10068	0.0014	3.7
	"-4.1 - -1.6"	3626614	10145	0.0028	
	"-1.6 - 0.9"	3038143	8820	0.0029	
	"0.9 - 4.0"	3293623	8910	0.0027	
	"4.0 - 13.8"	462213	1360	0.0029	
NDWI	"-0.40 - -0.19"	1092174	181	0.0002	26.4
	"-0.19 - -0.13"	3160641	3629	0.0011	
	"-0.13 - -0.10"	7815858	7537	0.0010	
	"-0.10 - -0.03"	4675414	12408	0.0027	
	"-0.03 - 0.1"	666463	15549	0.0233	
NDVI	"-0.155 - 0.0"	534759	15094	0.0282	27.1
	"0.0 - 0.06"	6682280	9112	0.0014	
	"0.06 - 0.1"	7348072	10641	0.0014	
	"0.1 - 0.2"	2142970	4315	0.0020	
	"0.2 - 0.4"	702469	142	0.0002	
	0-15.8	9338262	39098	0.0042	27.1

Distance to Stream (km)	15.8-39.7	2943230	204	0.0007	
	39.7-66.1	1968780	0	0.0000	
	66.1-96.1	1590039	0	0.0000	
	96.1-129.6	1570197	0	0.0000	
Curvature	-172,368,003,100 - -108,864,002,500	135704	144	0.0011	6.4
	-108,864,002,400 - -45,360,001,840	5020069	9513	0.0019	
	-45,360,001,830 - 18,143,998,770	7159844	20182	0.0028	
	18,143,998,780 - 81,647,999,390	4878194	9211	0.0019	
	81,647,999,400 - 145,152,000,000	216739	253	0.0012	

causative factors. Elevation, on the other hand, carries the lowest weight (0.0001). As a result, compared to the other components, elevation has a negligible contribution to flood incidence.

The soil texture of the study area consists of Loam, Loamy Sand, Clay Loam and Sandy Loam weighted 0.01, 0.01, 0.9 and 0.06, respectively. According to this notion, the clay loam is the major factor affecting flooding due to significant positive weight and loam and loamy sand are the least. Soils containing a significant proportion of clay typically exhibit slower infiltration rates and increased water holding capacities. As a result, they can absorb and retain a greater amount of water before producing runoff.

The literature analysis revealed that distance to stream had a significant impact on the likelihood of floods. Only the first class of distance to the stream (0 to 15.8 km) had a positive weight, according to the analysis, whereas the remaining classes had negative weights. This implies that as the distance from the river increases, the weight reduces, indicating that the farthest away from the river, the likelihood of flooding lowers. In other words, the farthest the areas from the streams (water bodies) the lower the risk of flooding.

The pattern of the influence of rainfall factor revealed that as rainfall increased, weights decreased, indicating a decreased risk of flooding with increased precipitation. In sandy desert regions, there is a probability where the areas with the highest average annual rainfall often experience reduced flood risks. This phenomenon can be attributed to the high impermeability of the sand, which efficiently absorbs a significant portion of the precipitation.

A flood susceptibility map is created by applying the FR and SE models. This map is created using the equation in raster calculator:

$$\text{FSI} = 0.0706 * \text{SLOPE}_{\text{FR}} + 0.0001 * \text{ELEVATION}_{\text{FR}} + 0.1630 * \text{RAINFALL}_{\text{FR}} + 0.1523 * \text{SOIL}_{\text{FR}} + 0.1057 * \text{LULC}_{\text{FR}} + 0.0797 * \text{GEOLOGY}_{\text{FR}} + 0.0036 * \text{TWI}_{\text{FR}} + 0.1257 * \text{NDWI}_{\text{FR}} + 0.1321 * \text{NDVI}_{\text{FR}} + 0.1584 * \text{STREAM DISTANCE}_{\text{FR}} + 0.0082 * \text{CURVATURE}_{\text{FR}}$$

Each raster cell's "flood susceptibility index" was assessed, and the results are shown on the map in Figure 3.14. The natural break approach was employed to create the flood susceptibility classifications, which are following: very low (2.6–24.7), low (24.7 – 51.7), moderate (51.7–79.2), high (79.2– 106.1) and very high susceptibility (106.1–140.1).

Figure 3.15 describes the spatial distribution of the flood susceptibility identified using SE Model. According to the chart 7% of the area is very high, 27% is high, 6% is moderate, 15% is low, and 45% is very low for flood susceptibility. A careful inspection indicates that the very high areas are the ones adjacent to the river Indus and similarly the high areas are the ones that contain the stream channels and zone showing very low flood susceptibility are the area of the Thar Desert.

The coarse source of flood was the rainfall which causes the rivers to overflow which intern then enables the stream channels in the study area to show the tendency of flash floods.

3.4 Analytical Hierarchy Process

The AHP is well known for being a very efficient approach to the MCDM process. It is frequently used to assess the relative importance of each criterion or element considered in the investigation. This strategy has been effectively used in several earlier research to weight flood causative elements, which finally led to the identification and mapping of flood-prone locations (Nagese et al, 2022).

3.5 Weight Linear Combination Approach

The relative importance of each causative factor and its associated weights were determined as part of the weighted linear combination approach's main steps. Based on actual information and contemporary research, the relative relevance of the chosen causative factors was determined, with a scale ranging from 7 (highest important) to 1 (lowest importance). Pairwise comparisons of the causative factors were evaluated based on

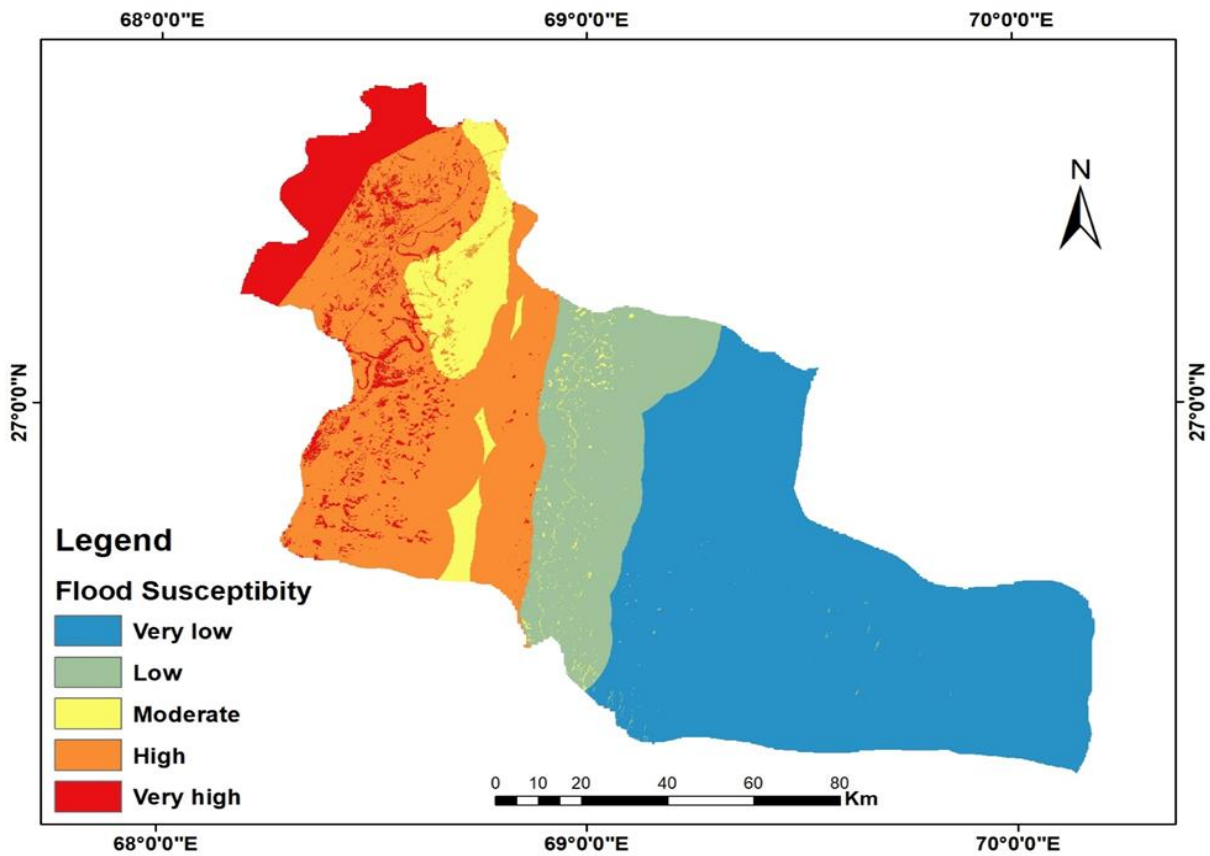


Figure 3.15. Flood susceptible zones using shannon's entropy.

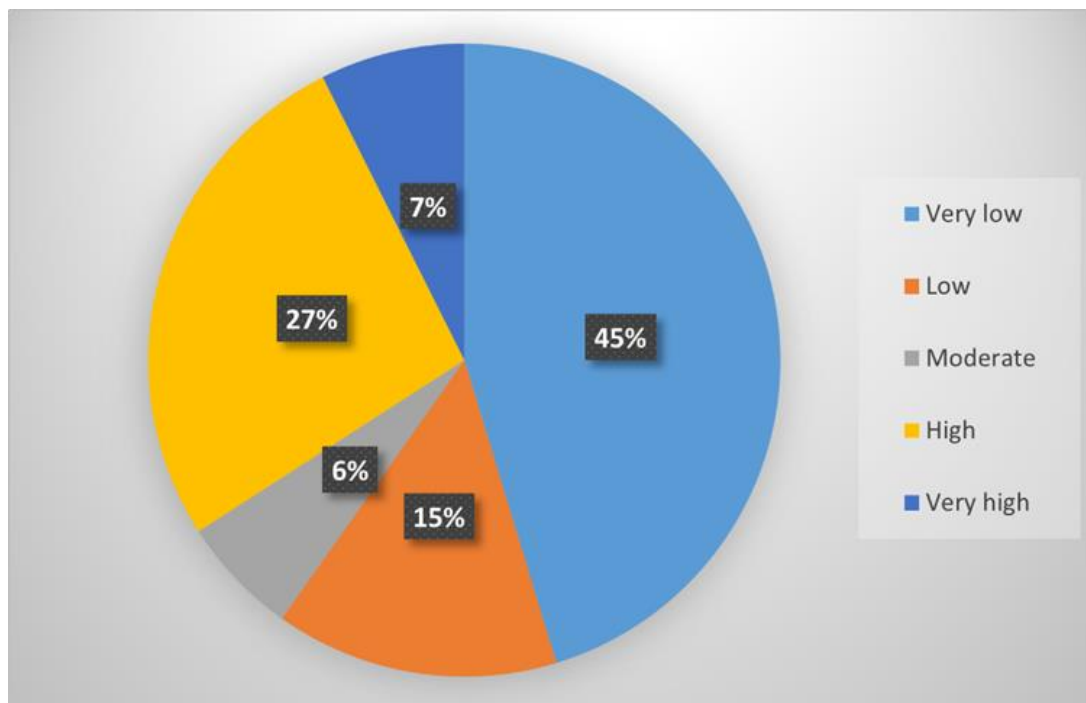


Figure 3.14. The calculated area of flood susceptibility zones.

Table 3.2. Shannon's entropy weights for each parameter.

Parameter	Classes	FR	E _{ij}	I _j	1-I _j	V _j
Slope (Degree)	0-3.9	0.0039	0.6138	-0.1301	0.3328	0.0707
	3.9-7.8	0.0015	0.2343	-0.1477		
	7.8-12.9	0.0005	0.0863	-0.0918		
	12.9-20.7	0.0002	0.0391	-0.0550		
	>20.7	0.0002	0.0265	-0.0418		
Elevation (m)	0-23	0.0021	0.1839	-0.1353	0.0008	0.0002
	23-68	0.0023	0.2020	-0.1403		
	68-111	0.0023	0.1963	-0.1388		
	111-152	0.0024	0.2024	-0.1404		
	152-180	0.0025	0.2155	-0.1436		
Rainfall (mm)	0.6-5.7	0.0058	0.9070	-0.0385	0.7677	0.1630
	5.7-11.2	0.0003	0.0492	-0.0644		
	11.2-17.7	0.0003	0.0438	-0.0595		
	17.7-23.8	0	0	0		
	23.8-30.1	0	0	0		
Soil	Loam	0.0005	0.0163	-0.02913	0.7177	0.1524
	Loamy Sand	0.0004	0.0131	-0.02470		
	Clay Loam	0.0301	0.9056	-0.03899		
	Sandy Loam	0.0022	0.0650	-0.07713		
LULC	Built-up	0.0059	0.1122	-0.1066	0.4982	0.1058
	Water	0.0411	0.7761	-0.0855		
	Vegetation	0.0058	0.1101	-0.1055		
	Barren Land	0.0001	0.0016	-0.0046		
Geology	Quaternary Sediments	0.0057	0.7383	-0.0973	0.3754	0.0797
	Quaternary Sand and Dune	0.0003	0.0397	-0.0556		
	Paleogene Sedimentary Rock	0.0017	0.2220	-0.1451		
TWI	"-8.1 - -4.1"	0.0014	0.1129	-0.1070	0.0171	0.0036
	"-4.1 - -1.6"	0.0028	0.2187	-0.1444		
	"-1.6 - 0.9"	0.0029	0.2269	-0.1462		
	"0.9 - 4.0"	0.0027	0.2115	-0.1427		
	"4.0 - 13.8"	0.0029	0.2300	-0.1468		
NDWI	"-0.40 - -0.19"	0.0002	0.0059	-0.0131	0.5924	0.1258
	"-0.19 - -0.13"	0.0011	0.0406	-0.0565		
	"-0.13 - -0.10"	0.0010	0.0341	-0.0501		
	"-0.10 - -0.03"	0.0027	0.0939	-0.0965		
	"-0.03 - 0.1"	0.0233	0.8255	-0.0688		
NDVI	"-0.155 - 0.0"	0.0282	0.8488	-0.0604	0.6226	0.1322
	"0.0 - 0.06"	0.0014	0.0410	-0.0569		

	"0.06 - 0.1"	0.0014	0.0435	-0.0593		
	"0.1 - 0.2"	0.0020	0.0606	-0.0737		
	"0.2 - 0.4"	0.0002	0.0061	-0.0135		
Distance to River (km)	0-15.8	0.0042	0.8580	-0.0571	0.7461	0.1584
	15.8-39.7	0.0007	0.1420	-0.1204		
	39.7-66.1	0	0	0		
	66.1-96.1	0	0	0		
	96.1-129.6	0	0	0		
Curvature	-172,368,003,100 - -108,864,002,500	0.0011	0.1202	-0.1106	0.0390	0.0083
	-108,864,002,400 - -45,360,001,840	0.0019	0.2146	-0.1434		
	-45,360,001,830 - 18,143,998,770	0.0028	0.3192	-0.1583		
	18,143,998,780 - 81,647,999,390	0.0019	0.2138	-0.1433		
	81,647,999,400 - 145,152,000,000	0.0012	0.1322	-0.1162		

professional judgement and information from the literature to determine the weights for each parameter. The approximation approach was then used to determine the normalized pairwise comparison matrix and the final weights, as shown in Table 3.5.

The final criterion weights given to each flood parameter are shown in Table 3.5, reflecting their relative impact on the likelihood of flooding in the study area.

The results reveal that distance to stream, precipitation and slope are the most significant factors in flood generation and curvature is the least.

The final flood susceptibility map was generated after applying the weighting total of all parameters. The natural break approach was employed to classify the final flood susceptibility map, as shown in Figure 3.16. Distance to Stream, Rainfall and Slope were observed as the most contributing factors in the derived map, and curvature the least. Figure 3.17 shows the flood susceptibility identified using AHP. According to the chart 23% of the area is very high, 15% is high, 16% is moderate, 19% is low, and 27% is very low for flood susceptibility. A careful inspection indicates that the very high areas are the ones adjacent to the river Indus and similarly the high areas are the ones that contain the stream channels, and the Thar Desert falls in very low flood susceptibility.

It is clear from the data in Table 3.6 that the FR map (45.2%) and the SE map (45.3%) have the highest proportions of the region designated as very low flood susceptibility. The AHP approach, on the other hand, produces the largest proportion of the region with a very high susceptibility (23.2%). The results indicate that, in comparison to the AHP map, the FR map and SE map show greater correspondence with each other. The three models flood susceptibility maps show a generally similar pattern, though some differences exist.

Table 3.3. Shows pair wise comparison matrix.

Factors	Elevation	Slope	NDWI	Rainfall	Distance to stream	Geology	TWI	LULC	Soil type	NDVI	Curvature
Elevation	1	1	1	1	1	2	3	2	3	2	2
Slope	1	1	3	3	1	3	3	1	3	3	5
NDWI	1	1	1	1	1	3	1	1	3	1	3
Rainfall	1	1/3	1	1	3	2	3	2	3	4	5
Distance to stream	1	1	1	1/3	1	7	7	7	7	7	7
Geology	1/2	1/3	1/3	1/2	1/7	1	1	1	1	1	1
TWI	1/3	1/3	1	1/3	1/7	1	1	1	2	3	4
LULC	1/2	1	1	1/2	1/7	1	1	1	2	3	4
Soil type	1/3	1/3	1/3	1/3	1/7	1	1/2	1/2	1	2	3
NDVI	1/2	1/3	1	1/4	1/7	1	1/3	1/3	1/2	1	2
Curvature	1/2	1/5	1/3	1/5	1/7	1	1/4	1/4	1/3	1/2	1
Sum	7.67	6.87	11.00	8.45	7.86	23.00	21.08	17.08	25.83	27.50	37.00

Table 3.4. Shows weightages of normalized factors.

Factors	Elevation	Slope	NDWI	Rainfall	Distance to stream	Geology	TWI	LULC	Soil type	NDVI	Curvature	Criteria Weights
Elevation	0.1304	0.1456	0.0909	0.1183	0.1273	0.0870	0.1423	0.1171	0.1161	0.0727	0.0541	0.1093
Slope	0.1304	0.1456	0.2727	0.3550	0.1273	0.1304	0.1423	0.0585	0.1161	0.1091	0.1351	0.1566
NDWI	0.1304	0.1456	0.0909	0.1183	0.1273	0.1304	0.0474	0.0585	0.1161	0.0364	0.0811	0.0984
Rainfall	0.1304	0.0485	0.0909	0.1183	0.3818	0.0870	0.1423	0.1171	0.1161	0.1455	0.1351	0.1376
Distance to stream	0.1304	0.1456	0.0909	0.0394	0.1273	0.3043	0.3320	0.4098	0.2710	0.2545	0.1892	0.2086
Geology	0.0652	0.0485	0.0303	0.0592	0.0182	0.0435	0.0474	0.0585	0.0387	0.0364	0.0270	0.0430
TWI	0.0435	0.0485	0.0909	0.0394	0.0182	0.0435	0.0474	0.0585	0.0774	0.1091	0.1081	0.0622
LULC	0.0652	0.1456	0.0909	0.0592	0.0182	0.0435	0.0474	0.0585	0.0774	0.1091	0.1081	0.0748
Soil type	0.0435	0.0485	0.0303	0.0394	0.0182	0.0435	0.0237	0.0293	0.0387	0.0727	0.0811	0.0426
NDVI	0.0652	0.0485	0.0909	0.0296	0.0182	0.0435	0.0158	0.0195	0.0194	0.0364	0.0541	0.0401
Curvature	0.0652	0.0291	0.0303	0.0237	0.0182	0.0435	0.0119	0.0146	0.0129	0.0182	0.0270	0.0268

3.6 Validation of The Flood Susceptibility Maps

It is important to have a clear and accurate record of the previous flood events to create flood susceptibility maps (Merz et al, 2007). An important part in every modelling process is accuracy assessment. The “AUC (Area Under Curve)” method is commonly employed in natural hazard studies because of its thorough, rational, and easily understandable validation technique (Nefeslioglu et al, 2010). AUC generates a range of values from 0 to 1. The AUC value increases toward 1, the methods accuracy increases, AUC value is 1 indicates the method is 100% effective (Tehrany et al, 2018).

The AUC has been computed based on true positive rates indicate flood points and false positive rate indicate the output of the model that is being tested. The black line in graph is reference line and defines true positive rate is equal to false positive rate and the red line is AUC curve. The effectiveness and performance of the three models FR, SE, and AHP were assessed in this study using the AUC method.

The AUC value for the FR, SE and AHP methods are shown in Fig.3.18, 3.19 and 3.20. AUC area results from the computation of each model are summarized in Table 3.6. The AUC values were 90.7%, 87.6%, and 79.5% for the FR, SE, and AHP models, respectively. The results show that the FR model provides the highest accuracy (90.7%). The flood susceptibility maps generated using the other models also exhibit considerable accuracy.

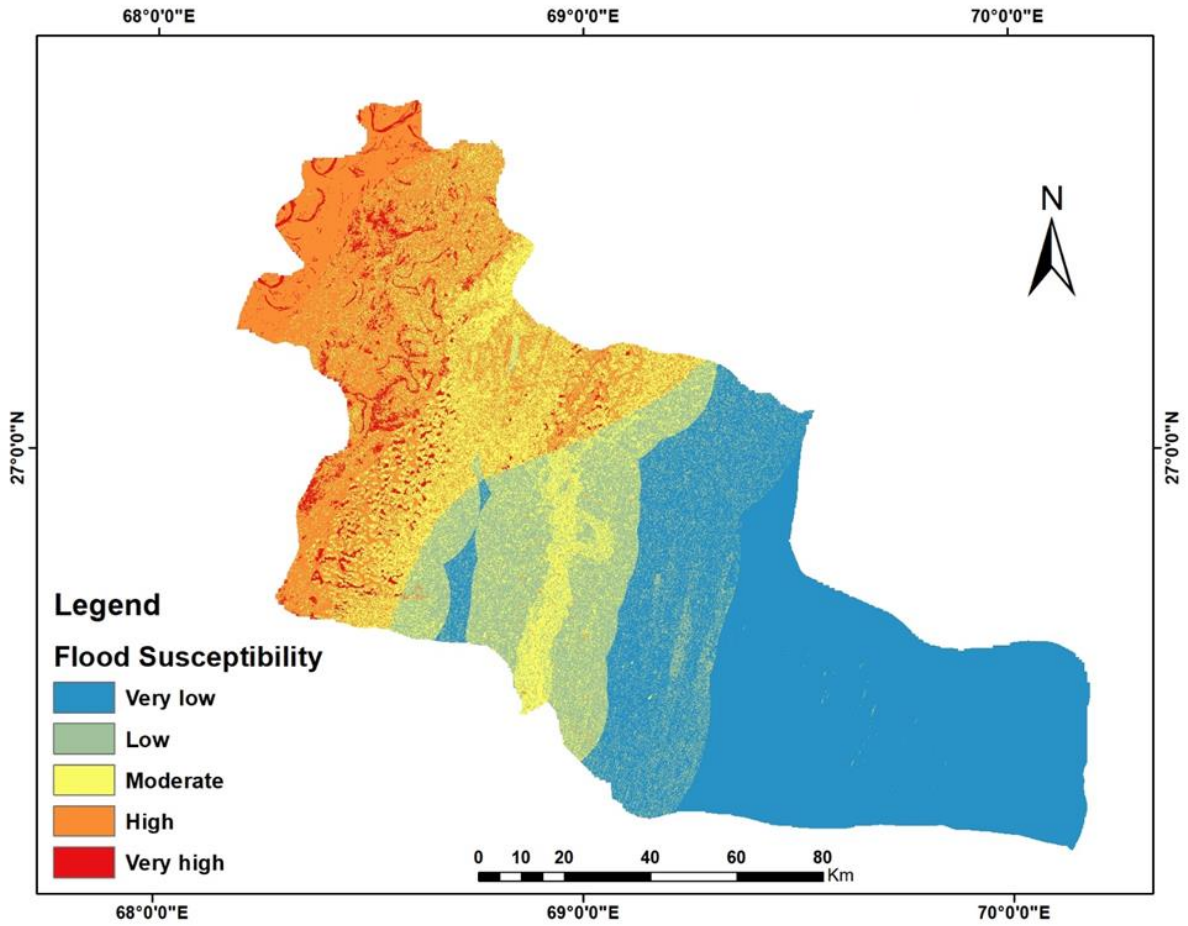


Figure 3.17. Flood susceptible zones using analytical hierarchy process model.

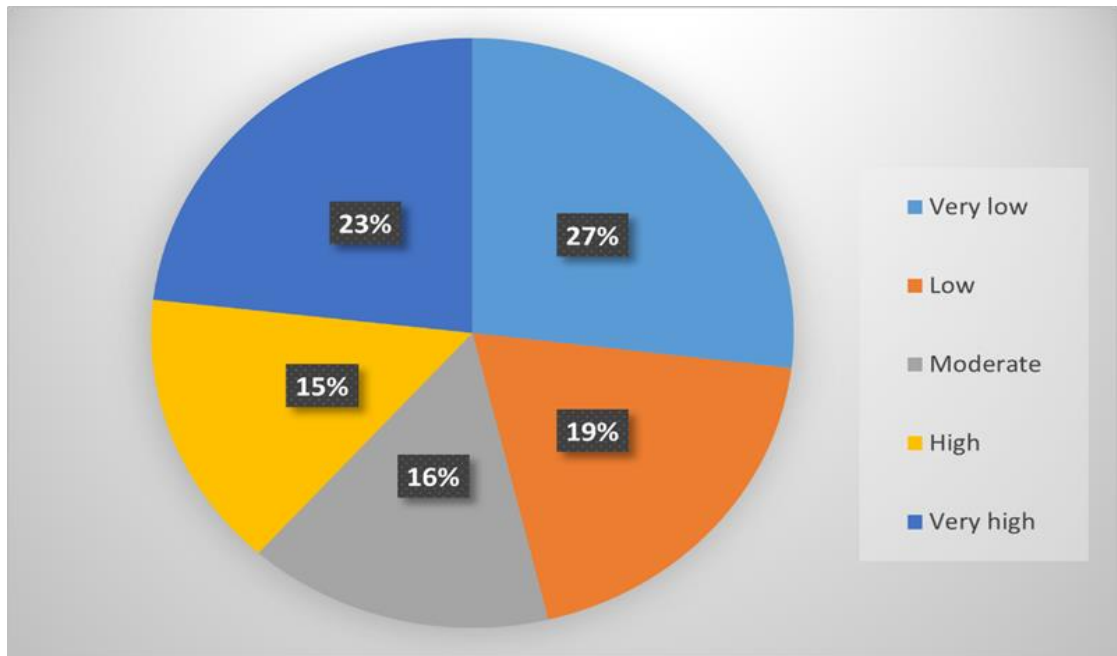


Figure 3.16. Distribution of flood susceptibility areas.

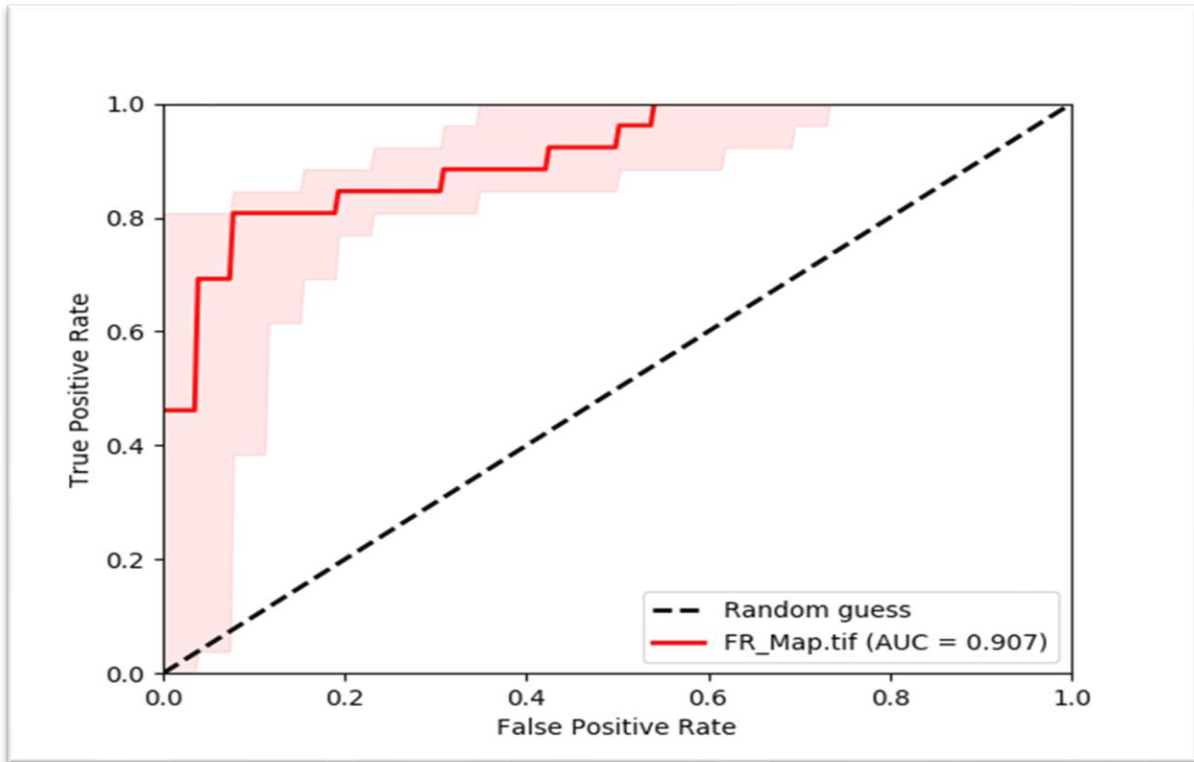


Figure 3.19. Area under curve representing quality of frequency ratio model.

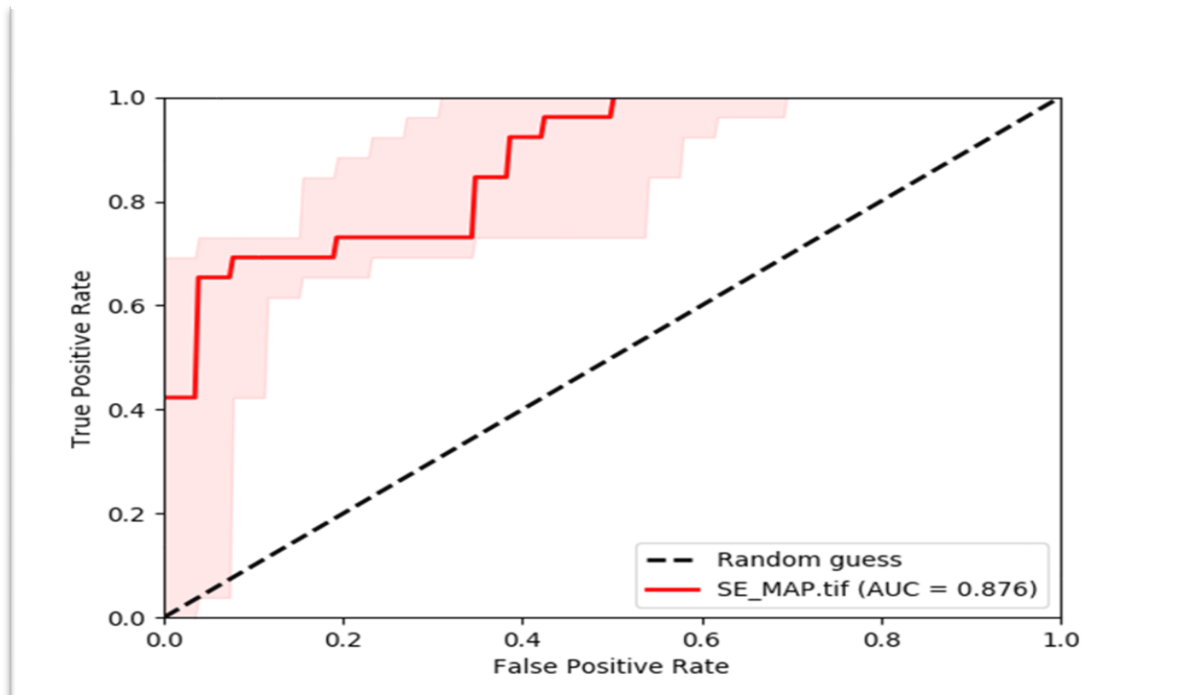


Figure 3.18. Area under curve representing quality of Shannon Entropy model.

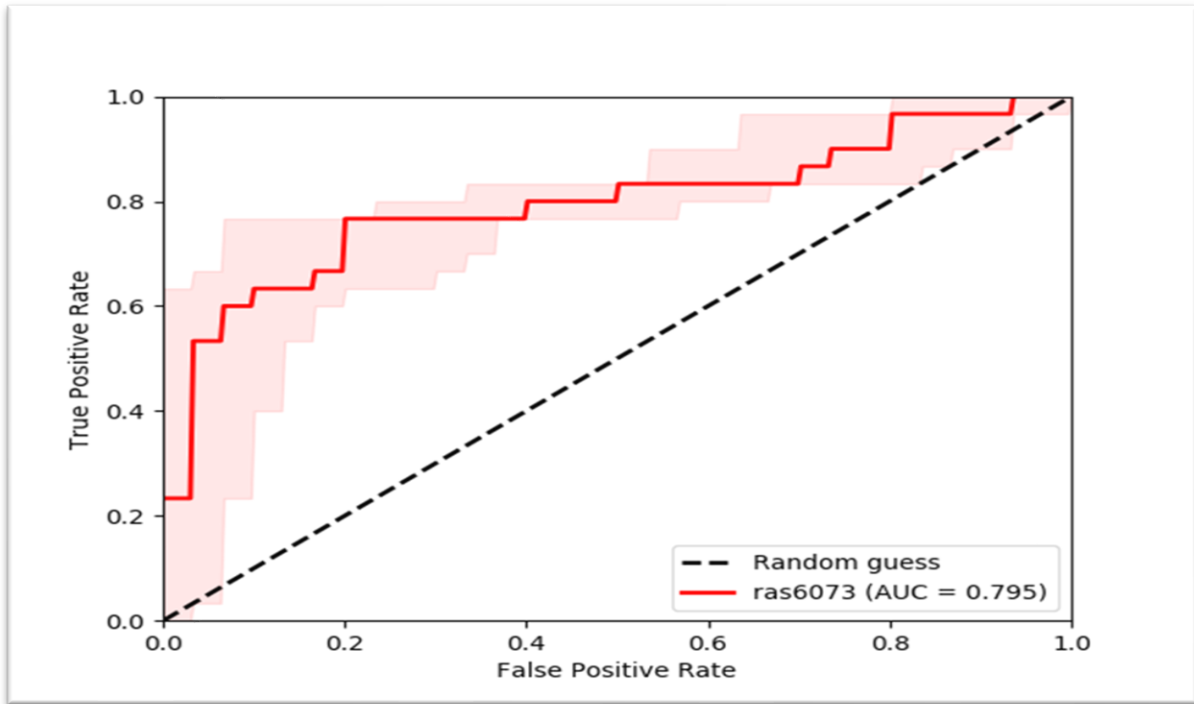


Figure 3.20. Area under curve representing quality of Analytical Hierarchy Process model.

Table 3.5. Area under curve values of models.

Model	AUC value (%)
Frequency Ratio	90.7
Shannon's Entropy	87.6
Analytic Hierarchy Process	79.5

CONCLUSION AND RECOMMENDATIONS

4.1 Conclusion

The delineation of flood-prone regions is a significant concern for water resources and land use planning and management. Over the past few years, various GIS based methods for mapping flood susceptibility have been developed and evaluated at different spatial extents. Flood susceptible maps play an important role in flood prevention and management. They provide valuable information about areas that are at risk of flooding and are used in several ways to enhance flood prevention efforts.

This study focused on the use of (FR), (SE) and (AHP) for the identification and mapping of flood susceptible areas in the study area. District Khairpur was selected due to major devastating floods occurrences in 2010 and 2022. These models are employed to examine the relationships between the spatial distributions of floods and certain independent variables (referred to as flood causative parameters) that determine the topography and hydrological features of the study area. For flood susceptibility mapping, eleven flood causative parameters were taken into consideration, including Elevation, Slope, Curvature, Topographic wetness index, NDVI, NDWI, LULC, Distance to stream, Average annual rainfall, Soil, and Geological map. Grid maps are created for each of these factors and then processed using GIS tools. The flood dataset consists of 125 flood events. For model, 70% of this data were utilized for model training, while 30% for model validation. The results reveal that distance to stream, precipitation and soil are the most important components in the generation of floods, and elevation the least significant for flood susceptibility in the study area. Comparing the results, in both the FR map and SE map, the highest proportion of the area is identified as having very low flood susceptibility, with percentages of 45.2% and 45.3%,

respectively. However, with the AHP method, the highest proportion of the area shows a very high susceptibility to flooding, with a value of 23.2%. The results reveal that FR map and SE map are correlated to each other as compared to AHP map. The flood susceptibility maps generated by the three models exhibit a comparable pattern, yet certain differences can be observed.

The validation procedure of the applied models is conducted by comparing the historical flood locations of the different flood susceptible zones on the final maps using “AUC (Area Under Curve)” Method. The AUC values were 90.7%, 87.6%, and 79.5% for the FR, SE, and AHP models, respectively. The results show that the FR model provides the highest accuracy (90.7%). The flood susceptibility maps produced by the other models also demonstrate a considerable level of accuracy.

The suggested maps can serve as valuable aids for water resource planners and decision-makers in land use management and planning. Particularly, flood susceptibility maps can play a crucial role to delineate flood prone areas where urbanization growth should be closely monitored or restricted to mitigate potential damage and losses from future floods.

4.2 Recommendations

To drive the maximum results from applied models, the models are usually calibrated using flood maps or historical flood events but unfortunately the imagery of the peak events was not available, nor it was possible to setup a field survey due to devastation of floods. Therefore, it is recommended to use the spatial extent of the extreme flood events for future disaster and risk management.

In this study the use of 30m SRTM DEM resolution was a limitation that can be overcome in future studies for planning a management using high resolution DEM imagery. Since the study area contains narrow rivers and stream channels the coarse resolution DEM

was bit of a challenge which limits the flood modelling process. Furthermore, the terrain is flat thus 30m DEM is not recommended for small rivers through plane area.

REFERENCES

1. Ahmad, B., Kaleem, M. S., Butt, M. J., & Dahri, Z. H. (2010). Hydrological modelling and flood hazard mapping of Nullah Lai. *Proc. Pakistan Acad. Sci*, 47(4), 215-226.
2. Al-Abadi, A. M., & Pradhan, B. (2020). In flood susceptibility assessment, is it scientifically correct to represent flood events as a point vector format and create flood inventory map. *Journal of Hydrology*, 590, 125475.
3. Balogun, A. L., Sheng, T. Y., Sallehuddin, M. H., Aina, Y. A., Dano, U. L., Pradhan, B., ... & Tella, A. (2022). Assessment of data mining, multi-criteria decision making and fuzzy-computing techniques for spatial flood susceptibility mapping: A comparative study. *Geocarto International*, 37(26), 12989-13015.
4. Chaudhri, S. A. (1981, October). Flood characteristics and problems in Pakistan. In *Natural Resources Forum* (Vol. 5, No. 4, pp. 399-407).
5. Chen, W., Li, W., Chai, H., Hou, E., Li, X., & Ding, X. (2016). GIS-based landslide susceptibility mapping using analytical hierarchy process (AHP) and certainty factor (CF) models for the Baozhong region of Baoji City, China. *Environmental Earth Sciences*, 75, 1-14.
6. Choi, J., Oh, H. J., Lee, H. J., Lee, C., & Lee, S. (2012). Combining landslide susceptibility maps obtained from frequency ratio, logistic regression, and artificial neural network models using ASTER images and GIS. *Engineering geology*, 124, 12-23.
7. Danso-Amoako, E., Scholz, M., Kalimeris, N., Yang, Q., & Shao, J. (2012). Predicting dam failure risk for sustainable flood retention basins: A generic case study for the wider Greater Manchester area. *Computers, Environment and Urban Systems*, 36(5), 423-433.
8. Das, S. (2020). Flood susceptibility mapping of the Western Ghat coastal belt using multi-source geospatial data and analytical hierarchy process (AHP). *Remote Sensing Applications: Society and Environment*.
9. Deen, S. (2015). Pakistan 2010 floods. Policy gaps in disaster preparedness and response. *International journal of disaster risk reduction*, 12, 341-349.
10. Eccles, R., Zhang, H., & Hamilton, D. (2019). A review of the effects of climate change on riverine flooding in subtropical and tropical regions. *Journal of Water and Climate Change*, 10(4), 687-707.
11. Hammami, S., Zouhri, L., Souissi, D., Souei, A., Zghibi, A., Marzougui, A., & Dlala, M. (2019). Application of the GIS based multi-criteria decision analysis and analytical hierarchy process (AHP) in the flood susceptibility mapping (Tunisia). *Arabian Journal of Geosciences*, 12, 1-16.
12. Islam, S., Tahir, M., & Parveen, S. (2022). GIS-based flood susceptibility mapping of the lower Bagmati basin in Bihar, using Shannon's entropy model. *Modeling Earth Systems and Environment*, 1-15.

13. Jothibas, A., & Anbazhagan, S. (2016). Flood susceptibility appraisal in Ponnaiyar River Basin, India using frequency ratio (FR) and Shannon's Entropy (SE) models. *Int J Adv Rem Sens GIS*, 5(10), 1946-1962.
14. Khan, F. A., Ali, J., Ullah, R., & Ayaz, S. (2013). Bacteriological quality assessment of drinking water available at the flood affected areas of Peshawar. *Toxicological & Environmental Chemistry*, 95(8), 1448-1454.
15. Khosrokhani, M., & Pradhan, B. (2014). Spatio-temporal assessment of soil erosion at Kuala Lumpur metropolitan city using remote sensing data and GIS. *Geomatics, Natural Hazards and Risk*, 5(3), 252-270.
16. Khan, I., Lei, H., Shah, A. A., Khan, I., & Muhammad, I. (2021). Climate change impact assessment, flood management, and mitigation strategies in Pakistan for sustainable future. *Environmental Science and Pollution Research*, 28, 29720-29731.
17. Khosravi, K., Pourghasemi, H. R., Chapi, K., & Bahri, M. (2016). Flash flood susceptibility analysis and its mapping using different bivariate models in Iran: a comparison between Shannon's entropy, statistical index, and weighting factor models. *Environmental monitoring and assessment*.
18. Kundzewicz, Z. W. (2014). Adapting flood preparedness tools to changing flood risk conditions: the situation in Poland. *Oceanologia*, 56(2), 385-407.
19. Liuzzo, L., Sammartano, V., & Freni, G. (2019). Comparison between different distributed methods for flood susceptibility mapping. *Water Resources Management*, 33, 3155-3173.
20. Chander, G., Markham, B. L., & Helder, D. L. (2009). Summary of current radiometric calibration coefficients for Landsat MSS, TM, ETM+, and EO-1 ALI sensors. *Remote sensing of environment*, 113(5), 893-903.
21. Marchi, L., Borga, M., Preciso, E., & Gaume, E. (2010). Characterisation of selected extreme flash floods in Europe and implications for flood risk management. *Journal of Hydrology*, 394(1-2), 118-133.
22. Msabi, M. M., & Makonyo, M. (2021). Flood susceptibility mapping using GIS and multi-criteria decision analysis: A case of Dodoma region, central Tanzania. *Remote Sensing Applications: Society and Environment*, 21.
23. Msabi, M. M., & Makonyo, M. (2021). Flood susceptibility mapping using GIS and multi-criteria decision analysis: A case of Dodoma region, central Tanzania. *Remote Sensing Applications: Society and Environment*, 21.
24. Mirza, M. M. Q. (2011). Climate change, flooding in South Asia and implications. *Regional environmental change*, 11(Suppl 1), 95-107.
25. Mustafa, D. (2002). Linking access and vulnerability: Perceptions of irrigation and flood management in Pakistan. *The Professional Geographer*, 54(1), 94-105.
26. Molla, H. R. (2011). Embankment of lower Ajoy River and its impact on brick-kiln industry in Central Bengal, India. *International Journal of Research in Social Sciences & Humanities*.

27. Merz, B., Thielen, A. H., & Gocht, M. (2007). Flood risk mapping at the local scale: concepts and challenges. *Flood risk management in Europe: innovation in policy and practice*, 231-251.
28. Manzoor, Z., Ehsan, M., Khan, M. B., Manzoor, A., Akhter, M. M., Sohail, M. T., & Abioui, M. (2022). Floods and flood management and its socio-economic impact on Pakistan: A review of the empirical literature. *Frontiers in Environmental Science*, 10.
29. Naghibi, S. A., Pourghasemi, H. R., Pourtaghi, Z. S., & Rezaei, A. (2015). Groundwater qanat potential mapping using frequency ratio and Shannon's entropy models in the Moghan watershed, Iran. *Earth Science Informatics*, 8, 171-186.
30. Nefeslioglu, H. A., Sezer, E. B. R. U., Gokceoglu, C., Bozkir, A. S., & Duman, T. Y. (2010). Assessment of landslide susceptibility by decision trees in the metropolitan area of Istanbul, Turkey. *Mathematical Problems in Engineering*, 2010.
31. Negese, A., Worku, D., Shitaye, A., & Getnet, H. (2022). Potential flood-prone area identification and mapping using GIS-based multi-criteria decision-making and analytical hierarchy process in Dega Damot district, northwestern Ethiopia. *Applied Water Science*, 12(12), 255.
32. Nied, M., Pardowitz, T., Nissen, K., Ulbrich, U., Hundecha, Y., & Merz, B. (2014). On the relationship between hydro-meteorological patterns and flood types. *Journal of Hydrology*, 519, 3249-3262.
33. Panchal, S., & Shrivastava, A. K. (2021). A comparative study of frequency ratio, Shannon's entropy and analytic hierarchy process (AHP) models for landslide susceptibility assessment. *ISPRS International Journal of Geo-Information*, 10(9), 603.
34. Poff, N. L. (2002). Ecological response to and management of increased flooding caused by climate change. *Philosophical transactions of the royal society of London. Series A: mathematical, physical and engineering sciences*, 360(1796), 1497-1510.
35. Pourghasemi, H. R., Pradhan, B., & Gokceoglu, C. (2012). Application of fuzzy logic and analytical hierarchy process (AHP) to landslide susceptibility mapping at Haraz watershed, Iran. *Natural hazards*, 63, 965-996.
36. Panchal, S., & Shrivastava, A. K. (2021). A comparative study of frequency ratio, Shannon's entropy and analytic hierarchy process (AHP) models for landslide susceptibility assessment. *ISPRS International Journal of Geo-Information*, 10(9), 603.
37. Rahmati, O., Pourghasemi, H. R., & Zeinivand, H. (2016). Flood susceptibility mapping using frequency ratio and weights-of-evidence models in the Golastan Province, Iran. *Geocarto International*, 31(1), 42-70.
38. Robert Looney (2012): Economic impacts of the floods in Pakistan, *Contemporary South Asia*, 20:2, 225-241.
39. Saaty, T. L. (1997). That is not the analytic hierarchy process: what the AHP is and what it is not. *Journal of Multi-Criteria Decision Analysis*, 6(6), 324-335.
40. Samu, R., & Kentel, A. S. (2018). An analysis of the flood management and mitigation measures in Zimbabwe for a sustainable future. *International journal of disaster risk reduction*, 31, 691-697.

41. Shafapour Tehrany, M., Kumar, L., Neamah Jebur, M., & Shabani, F. (2019). Evaluating the application of the statistical index method in flood susceptibility mapping and its comparison with frequency ratio and logistic regression methods. *Geomatics, Natural Hazards and Risk*, 10(1), 79-101.
42. Swain, K. C., Singha, C., & Nayak, L. (2020). Flood susceptibility mapping through the GIS-AHP technique using the cloud. *ISPRS International Journal of Geo-Information*, 9(12), 720.
43. Tabari, H. (2020). Climate change impact on flood and extreme precipitation increases with water availability. *Scientific reports*, 10(1), 13768.
44. Tariq, M. A. U. R., & Van De Giesen, N. (2012). Floods and flood management in Pakistan. *Physics and Chemistry of the Earth, Parts A/B/C*, 47, 11-20.
45. Tehrany, M. S., Pradhan, B., & Jebur, M. N. (2013). Spatial prediction of flood susceptible areas using rule based decision tree (DT) and a novel ensemble bivariate and multivariate statistical models in GIS. *Journal of hydrology*, 504, 69-79.
46. Vojtek, M., & Vojteková, J. (2019). Flood susceptibility mapping on a national scale in Slovakia using the analytical hierarchy process. *Water*, 11(2), 364.
47. Weissmann, G. S., Hartley, A. J., Nichols, G. J., Scuderi, L. A., Olson, M., Buehler, H., & Banteah, R. (2010). Fluvial form in modern continental sedimentary basins: distributive fluvial systems. *Geology*, 38(1), 39-42.
48. Wang, Y., Fang, Z., Hong, H., Costache, R., & Tang, X. (2021). Flood susceptibility mapping by integrating frequency ratio and index of entropy with multilayer perceptron and classification and regression tree. *Journal of Environmental Management*, 289.